World Journal of Advanced Engineering Technology and Sciences
eISSN: 2582-8266
Cross Ref DOI: 10.30574/wjaets
Journal homepage: https://wjaets.com/

(RESEARCH ARTICLE)

Check for updates

Geophysical, hydrogeological and laboratory assessment of groundwater quality and its health implication in some urban communities in cross river state

Atan Obeten Egor *

Department of Physics, Cross River University of Technology Calabar, Nigeria.

World Journal of Advanced Engineering Technology and Sciences, 2023, 10(02), 239–264

Publication history: Received on 30 October 2023; revised on 09 December 2023; accepted on 12 December 2023

Article DOI: https://doi.org/10.30574/wjaets.2023.10.2.0301

Abstract

The electrical resistivity technique which involved the Schlumberger depth sounding method, electrical resistivity tomography and geochemical analyses of water samples collected from boreholes were used to investigate the quality of groundwater in some urban communities in Cross River State, also the health implication of the said groundwater was also investigated. Forty nine electrical resistivity data were collected, modeled, and interpreted after calibration with lithologic logs. Ten electrical resistivity tomography data was were also collected, modeled and interpreted. Forty nine borehole water samples were collected and analyzed to determine anion, cation concentrations and some physical and chemical parameters, such as water colour, temperature, total dissolved solids, and electrical conductivity. The results show that the lithostratigraphy of the study area is composed of sands, sandstones (fractured, consolidated and loosed), siltstones, shales (compacted and fractured) of the Asu River Group, Eze-Aku Formation which comprises the aquifer units, and the Nkporo Shale Formation. The aquifer conduits are known to be rich in silicate minerals, and the groundwater samples in some locations show a significant amount of Ca^{2+}, Mg^{2+}, and Na^{+}. These cations balanced the consumption of H^{+} during the hydrolytic alteration of silicate minerals. The geochemical analysis of groundwater samples revealed dominant calcium–magnesium–carbonate– bicarbonate water faces. The groundwater quality was observed to be influenced by the interaction of some geologic processes but was classified to be good to excellent, indicating its suitability for domestic and irrigation purposes.

Keywords: Groundwater; Electrical sounding; Water facies; Physico-chemical; Electrostratgraphic

1. Introduction

The most desired and efficient source of water for home and agricultural purposes is groundwater. In West Africa's rural and urban areas, groundwater supply has greatly grown recently and has taken over as the primary source of water for all purposes, particularly during the dry season (Pimentel et al. 1997). Rivers, lakes, and dams are some of the surface water resources in this area that are influenced by the seasonal rainfall (Pimentel et al. 1997). Some metropolitan communities in Cross River State are aware of their growing water needs. Given that using contaminated surface water for domestic purposes increases the risk of developing several endemic health issues brought on by water-borne illnesses (such as guinea worm, cholera, and dysentery), we undertook this study to aid in the search for additional high-quality water resources. The majority of rural residents' water supplies are rivers, streams, ponds, and lakes, all of which are extremely vulnerable due to surface pollution brought on by human activity (Akpan et al. 2013). In collaboration with the government of Cross River State, a number of donor organizations (such as the United Nations Children's Emergency Fund, the European Union, the Micro Project Programme in the nine Niger Delta States, the Niger Delta Development Commission, and the Cross River State Community and Social Development Agency) have been active in a variety of capacities to address the looming problems with the people's access to water. These organizations have made concerted attempts to address these issues by supporting the installation of additional social amenities and the drilling of water boreholes in villages to lessen the suffering of the populace. Groundwater resources must be

* Corresponding author: Egor A. O

regularly assessed to determine whether they are suitable for the aforementioned uses because this is of utmost importance (Ketata et al. 2011).

According to hydrogeophysical studies conducted in the Calabar flank and Ikom Mamfe Embayment (IME) (Fig. 1), the groundwater resource is not distributed uniformly. While some regions have abundant supplies of this material, others are constrained as a result of the region's complicated geologic history (Ebong et al. 2014; Akpan et al. 2013). The embayment has faced significant threats over time due to the failure of water boreholes, the rapid depletion of groundwater in the majority of the area as a result of excessive abstraction, and contaminants from geologic formations, soils, and sediments, as well as anthropogenic sources (Papadopoulou-Vrynioti et al. 2013, 2014; Akpan et al. 2015; Egor et al 2016). In the study area, population growth and the expansion of industrial and agricultural activities led to an increase in the demand for water. Studies on groundwater quality in the Mamfe region and the Calabar flank, however, are largely regional in scope and don't appear to be pertinent for local scales. It is for this reason that the goal of our inquiry is to evaluate the suitability of groundwater from the aquifer system for both household and health-related uses in select urban districts in Cross River State. We combined the depth sounding technique, electrical resistivity tomography, and geochemical and hydrogeologic data in our work.

The depth sounding method has been used successfully to address a variety of hydrological, hydrogeophysical, engineering, and environmental issues, such as aquifer mapping and geohydraulic parameter estimation (Soupios et al. 2007; Massoud et al. 2010;

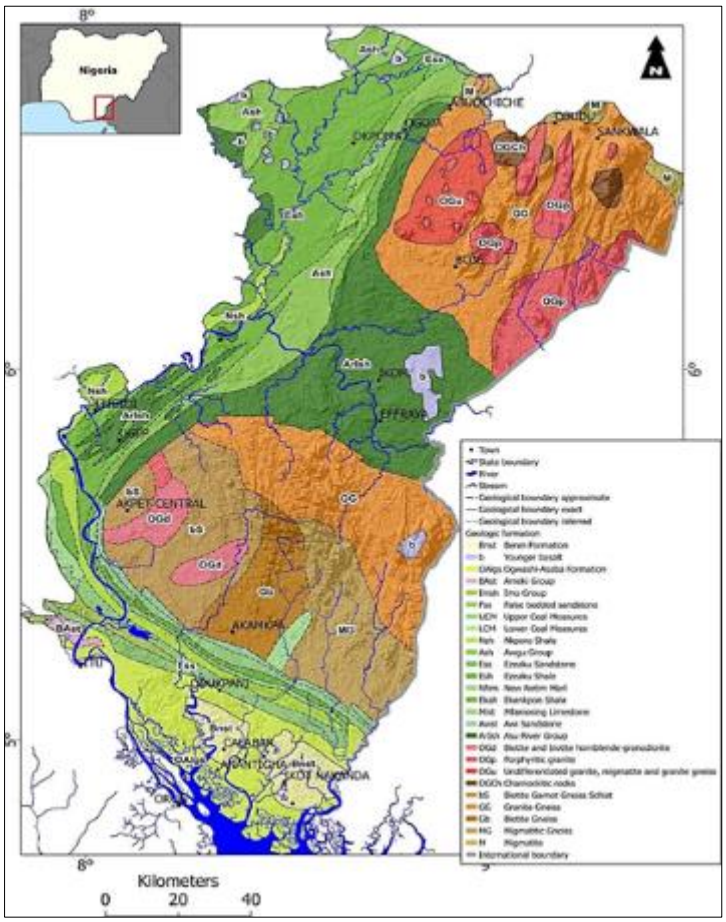

Figure 1 Geological Map of the Study Area

Ebong et al. 2014), characterizing aquifer formation, determining the rate at which the vadose zone infiltrates the groundwater, and groundwater contamination studies (Inoubli et al. 2006; Samsudin et al. 2007; Ogilvy et al. 2008; Gemail et al. 2011; Minsley et al. 2011; Akpan et al. 2013; Mhamdi et al. 2015; Egor et al 2016). Several authors have employed spatial geochemical data analyses with multiple criteria to estimate contamination levels in groundwater samples (Bathrellos et al. 2008; Panagopoulos et al. 2012). The major goal of this inquiry is to evaluate the quality, distribution, and availability of groundwater resources for household usage in several metropolitan communities in Cross River State, south-south Nigeria, as well as the potential health effects of ingesting the said groundwater.

1.1. Geological Setting

In Cross River State, Nigeria, the study area is situated between latitudes 5.76 and 6.02N and longitudes 7.93 and 8.17E. (Fig. 1b). The region is bordered to the north by Boki Local Government Area, to the northeast by Ebonyi State, and to the south by Akpabuyo Local Government Area and the Atlantic Ocean. The area which comprises of urban communities in Calabar Municipal, Calabar South, Odukpani, Akamkpa, Biase, Yakurr, Abi, Obubra, and Ikom Local Government Areas is located in the Ikom Manfe Embayment (IME) and the Calabar flank which extends between longitudes 7.75 and 8.75E and latitudes 5.25 and 6.50N (Akpan et al. 2013). Studies by Petters et al. (1987) revealed that the IME is always referred to as a contiguous component of the Lower Benue Trough and is the NW-SE splay segment of the NE-SW trending Benue Trough (LBT). The IME stretch of the LBT covers an area of 2016 km2 and veers laterally into portions of western Cameroun (Nguimbous-Kouoh et al. 2012; Egor et al 2020).

The Obudu Plateau and the Cameroun Volcanic Line form the northeast and western boundaries of the IME, respectively, as do the Abakaliki Anticlinorium and the Afikpo Syncline. The Oban Massif in Cross River State, Nigeria, forms its southern border (Fig. 1a). The IME traverses the Cross River State local government areas (LGAs) of Abi, Obubra, Yakurr, Biase, and Ikom and is distinguished by low relief and gently undulating landscape (Eseme et al. 2002). The Anambra Basin subsided as a result of the westward displacement of the depositional axis in the Benue Trough that followed the mid-Santonian tectonism and magmatism. Sediments from the Campanian-Maestrichtian to Eocene ages are found in the Anambra basin, which is a portion of the LBT, but not in the IME (Odigi 2011). (Fig. 1). The whole Benue Trough was subject to compressional folding during the mid-Santonian, which produced a number of formations like the Abakaliki Anticlinorium and Afikpo Syncline, which eventually evolved into Afikpo Basin (Benkhelil 1982).

Marine Albian Asu River Group (ARG), the first lithostratigraphic unit to rest irregularly on the Precambrian crystalline basement, is where the IME's sedimentation process got started (PCB). In general, the PCB is composed of migmatitic gneiss, granitic gneiss, and schist, with a few pegmatitic intrusions in specific places (Fig. 1). The gneisses in the PCB typically have pink feldspathic minerals foliated on them and range in color from black to white hornblende with porphyroclastic feldspars (Akpan et al. 2013; Ekwueme et al. 1995; Egor et al 2020). The regional striking direction of these rocks is N-S, while Odoh (2010) and Ekwueme also documented some sporadic NE-SW oscillations (2003). A few reports of pyroclastics from the Aptian to Early Albian period exist (Odigi and Amajor 2009). The nonmarine-to-marginal marine character sediments known as the ARG are made up of ammonite-rich limestones, impermeable shales, and sand lenses (Petters et al. 1987).

The Eze-Aku Group (EAG), which correlates with the marine Cenomanian-Turonian Nkalagu Formation (black shale, limestone, and siltstone), and the interfingering regressive sandstones of the Agala Formation, overlies the ARG. It is composed of thick, flaky, impermeable, calcareous and noncalcareous black shale, siltstone, and sandstone Locally, this formation's thickness does surpass 100 meters (Ukaegbu and Akpabio 2009). According to Murat (1972), the sandstone deposits marked a period of regression, whilst the shale deposits suggest a period of transgression. The Eze-Aku Shale represents deposits of marine condition in a tectonically controlled basin. These Tertiary volcanic rocks, such as basalts and dolerites in some places, are occasionally found intruding into these Cretaceous deposits (Benkhelil 1982). The nearby Cameroun Volcanic Province and other low-grade metamorphism in the region were thought to be the source of the post-Cretaceous tectonic events, which resulted in severe fracturing of the basement rocks and distortion of the nearby Cretaceous lithostratigraphic units (Ebong et al. 2014; Akpan et al. 2013; Egor et al 2020). As a result, the overlying Cretaceous sequence is severely distorted, heavily baked, and domed in numerous places (Etuk et al. 2008; Offodile 1975). The sandstones in the EAG produce ridges in numerous places, such as the Owutu-Afikpo-Adadama Ridge System (OAASRS), which typically strike at N400E and dip between 200 and 680. (Odigi and Amajor 2009). The post-Cretaceous tectonic events that caused extensive fractures in the basement rocks and distortion of the neighboring Cretaceous lithostratigraphic units were assumed to have originated from the nearby Cameroun Volcanic Province and other low-grade metamorphism in the area (Ebong et al. 2014; Akpan et al. 2013; Egor et al 2020). As a result, the Cretaceous sequence that lies above is greatly deformed, extensively baked, and dome-shaped in several locations (Etuk et al. 2008; Offodile 1975). The Owutu-Afikpo-Adadama Ridge System (OAASRS), which normally strikes about N400E and dips between 200 and 680, is one of many ridges produced by the sandstones in the EAG (Odigi and Amajor 2009).

The Calabar Flank is a sedimentary basin in South Eastern Nigeria that is bounded to the west by the enormous Oban Massif crystalline foundation group. The Ikang Trough, the Ituk High, and NW-SE trending are features of the subsurface (Reijers, 1998). The Calabar Hinge borders these features on the western arm (Figure 1). A wide variety of sedimentary rocks from the Cretaceous and more recent periods make up the Calabar Flank. The Upper Aptian-Albian Mfamosing Limestone Formation, Neocomian-Aptian Awi Formation, and Upper Ekenkpon and New Netim Shales make up the Cretaceous interval on the Calabar Flank (Akpan, 1990; Reijers and Peters, 1997). (Reijers, 1998). The Odukpani Group is comprised of the Awi and Mfamosing Formations. Based on basic volcanism and disconformity, it is thought that these

sedimentary rocks were deposited before the Santonian compressional tectonic phase (Reijers, 1998). The Campanian Nkporo shales, Tertiary marine shales, and regressive sandstone are located unevenly above this.

1.2. Hydrogeology

The quality of groundwater in aquifers is influenced by factors such as the quantity and duration of water, depth of weathering, specific yield, and slope of formation toward drainage channels (Srinivasamoorthy et al. 2014). Whether you are limited or not, it is still possible. The shallow aquifers (about 60 m) in the area were created by the high-level metamorphism and fracturing of the EAG. The main groundwater aquifers in the area are therefore made up of cracked sandstones, sand lenses, and siltstones (Ebong et al. 2014). Permeability estimates around the fractured shale and siltstone aquifers range from 2.0 to 3.0 m/day. The sandstone and cracked sandstone aquifers have permeabilities that range from 3.2 to 4.5 m/day. Aquifer depths vary from 7 to 27 meters, and daily transmissivity values range from 25 to 100 meters (Ebong et al. 2014). Local study suggests that high yielding aquifers could exist at depths more than 100 m. These aquifer structures are unique to this region (Akpan et al. 2013, 2015 The region has 2200 mm of annual precipitation and relative humidity on average, as well as average yearly temperatures that vary between 23 and 27 °C in the rainy season and peak at 35 °C in the dry season, all according to Akpan et al. (2013). (Ebong et al. 2014; Egor et al 2020). The main drainage system for the study region is made up of the Cross River, the Qua River, and its tributaries the Okwo and Okpon, which experience seasonal variations in water volume. Other smaller water inlets that are tributaries of the main river, such as rivers and streams, also drain the area (Cross River). When water levels in both surface and groundwater resources reach their highest during the height of the rainy season, the principal drain overflows its banks. Due to topographic pressures, as seepages from the OAASRS travel towards low-lying areas, the soil in these regions becomes saturated during the rainy season (Ebong et al. 2014). Localized evapotranspiration, localized water loss to surface waterways like ponds, and principally the main drain (Rivers and streams) to contain less water as the dry season comes to an end. The Cross River's water flow is restricted to minuscule channels within the riverbed at this time.

2. Material and methods

The research area includes urban areas in Calabar South, Calabar Municipal, Odukpani, Akamkpa Biase, Yakurr, Abi, Obubra, and Ikom Local Government Areas. The research area is the political and economic center of Cross River State and has a land area of 11480 square kilometers and a population of 1.7 million (Ushie et al 2014).

2.1. Water sampling

55 drinking water sources (boreholes) were sampled across the study area between June and August 2022. One sample was gathered from each borehole and put into sample bottles without additional processing in accordance with the accepted practices for gathering water and the risky consumer behaviors. The sampling strategy was carefully constructed to include samples from every area of the study zone due to financial constraints. Our sample approach employed purposeful random sampling, and the sampling sites were chosen from a group of such places. The sample crew interviewed the borehole owner, custodian, or a regular user at each sampling station to determine the age of the source, depth, and number of residences using the borehole. The water was then sampled, and two separate 250 ml sterilized glass sampling bottles—one for bacterial analysis and one for chemical analysis—were used (Ketata et al., 2011; Osang et al., 2016). The samples were then pumped or allowed to flow at full force for 10 minutes. The Hanna Instruments USA H198130 model of combination electrical conductivity (EC) and PH meter was used for in-situ measurements of physic-chemical parameters (EC, PH, TDS, and temperature) because these parameters vary with air conditions like temperature. In order to evaluate the concentration of. The Cross River State Water Board Limited (CRSWBL) a certified laboratory for water analysis received the sample bottles and conducted the bacterial examination first, followed by the chemical analysis of the metal samples.

2.2. Bacterial Analysis

In accordance with WHO (2011) standards, the total coliform and fecal contamination samples were examined using the membrane filtering method, in the Cross River State Water Board laboratory. The membrane filter paper (0.45-micrometer porosity) was placed inside the filter holder, which was fixed to a fund that was placed on top of a Buchner flask. 100 ml of the water sample was put to the funnel, where it was all vacuumed through the paper while being shaken. A sterile absorbent pad was placed in a sterile Petri dish, and 2ml of the nutritive medium was then added to the pad. After removing the water sample with sterile forceps, the filter paper was placed over the absorbent pad in the petri dish.

2.3. Chemical analysis

The concentrations of each inorganic chemical were determined at the CRSWBL Calabar. According to the Safe Drinking Water Act, the CRSWBL Laboratory is accredited by the Federal Environmental Laboratory Accreditation Program (FELAP) and the National Agency for Food and Drug Administrator Control (NAFDAC). It is also certified by the Nigerian Standard for Drinking-Water Quality (NSDWQ) (NSDWQ 2007).

The concentrations of aluminum, arsenic, barium (Ba), cadmium, chromium (Cr), copper, mercury, nickel (Ni), lead (Pb), and zinc were measured using an absorption atomic spectrophotometer. While the total hardness (CaCO3), calcium (Ca2+), carbonate (C032), bicarbonate (HCO3-), and chloride were all analyzed using the volumetric method, the concentration of Na+ and k+ was evaluated using a flame photometer (Cl-). (2017) Osang et al For this undertaking, the caliber

2.4. Household and Health Surveys

The use of household water was inquired about from at least 10 consecutive users of each of the 49 boreholes where samples were gathered. In addition, questions on their ages, health state, and the hospital or healthcare facility where the interviews were performed were asked. In a structured interview, trained student volunteers asked respondents about their usage of the source for drinking, their awareness of drinking, their awareness of water-borne illnesses, their opinions on the taste of the water, and why they picked it over other sources.

The questionnaire was presented since the survey instrument had a section designed to gather data on respondents' health state. Each participant was made aware of the study's goals, the fact that participation was completely optional, the fact that the study report would not contain any information that might be used to identify them, and the possibility of not responding to any questions before the start of each survey. The responders verbally consented before the interviews started. 3600 people's medical records from 550 families in total were included. The research team followed all ethical and scientific standards set forth by the Cross River University of Technology and the health ministry in conducting their research.

2.5. Analysis of Faecal Samples Using Formal Ether Concentration

The only individuals who contributed excrement for collecting were citizens, students, teachers, dumpsite personnel, restaurant proprietors, human scavengers, and other tiny traders and business owners. After that, these samples were examined utilizing Cheesebrangh's methodology (2006).

2.6. Geoelectrical data acquisition

The geoelectrical resistivity technique was used to conduct vertical electrical sounding (VES) and electrical resistivity tomography (ERT) investigations utilizing the wenner array and Schlumberger electrode configuration, respectively. The Schlumberger array is known to consistently provide shallow subsurface stratigraphic contrast. The method is carried out by connecting a resistivity meter to two sets of electrodes known as current and potential electrodes. The formula serves as the theoretical foundation for data collecting.

$$\rho_{as} = \frac{\pi b^2 R}{4a} = \frac{\pi\left(\frac{AB}{2}\right)^2 - \left(\frac{MN}{2}\right)^2}{MN}\frac{\Delta V}{I} \quad \ldots\ldots\ldots\ldots\ldots\ldots\ldots\ldots\ldots\ldots\ldots\ldots\ldots\ldots\ldots (1)$$

Where R is the apparent resistance, AB is the current electrode distance, MN is the potential electrode distance, V is the voltage, and I is current. _as is the Schlumberger apparent resistivity. Each sounding station's computed _as is always plotted against the present electrode spacing's half (AB/2), VES curves are obtained, and noisy parts are manually smoothed out (Bhattacharya, 1968; Chakravarthi et al., 2007; Osang et al 2017).

The survey was conducted using an IGIS resistivity meter (model SSR-MP-ATS). In order to correlate sounding data with lithological logs from the boreholes and aquifer protective capacities for the purposes of considering water quality, thirty (30) vertical electrical sounding were conducted in locations near to the boreholes where water samples had been taken. While the potential electrode spacing varies between 0.25 and 20m, the proper electrode spacing spans from a minimum of 2.m to a maximum of 500m. These parameters were selected to provide for the best mapping of both shallow and deeply seated structures (>100m). Considering that the electrode spacing is approximately 1/3 of the maximum current penetration.

So that observed resistances can be visually converted and compared with previous values at the same current electrode position, potential electrode values at cross-over points were carefully chosen to take on integer multiples of their previous values. Observed data were manually plotted in the field on a bi-logarithmic graph by plotting half-current electrode spacing on the abscissa against apparent resistivity (pa) on the ordinate axes, respectively. Before moving on to the next survey point, the exercise was performed to evaluate the caliber of data collected. When appropriate, standard curve matching and smoothing procedures were also used, and standard charts were used for qualitative interpretations (Orellana and moony 1966; Osang et al 2020).

The computer-aided modeling approach used the RESIST code created by Vender Velpen in 1988. The starting parameters for the inversion procedure, such as resistivities and depths, were determined from manically interpreted curves and restricted by lithological logs. The logs of lithology. The Cross River State Rural Water Supply and Sanitation Agency (CR-RUWATSSA), Fatigen Drilling Company, and Cross River State Community and Rural Development Agency provided the lithological logs from boreholes that were closest to the VES locations (CRSCRDA). The root-mean-square (RMS) method was used by the Resist program to compare the disparities between the field data and the synthetic models.

Noisy data sets frequently had high RMS errors, which were linked to poor ground contact. These noisy raw data were either manually smoothed or eliminated using software-built user-defined filtering criteria.

2.7. Electrical resistivity tomography data acquisition

ERT is carried out using a multi-electrode resistivity imaging instrument and effective data processing software built on inversion methods. Multiple multi-core cables with numerous electrode takeouts are joined together to produce a multi-electrode setup for ERT, allowing any four electrodes to be used (two for current injection and two for potential measurement). There are various numbers of electrodes in each system. 64 electrodes, 72 electrodes, and so on are possible for systems. Equipment for ERT has been produced by numerous global firms. This study makes use of the ABEM-developed SAS 3000 resistivity meter from the Terrameter Imaging System.

Four multi-core cables with 16 electrodes each are used in ERT. The two electrodes are separated by ten meters. This ERT unit's dispersion radius is 500 meters. If necessary, the distance between the electrodes can be shortened. In order to conduct an ERT survey, four multi-core cables with 16 evenly spaced electrodes on each are used. Depending on the type of survey, the distance between the electrodes can be changed. High-resolution imaging of the subsurface requires short distances. In order to connect an electronics witching unit, multi-core cables are utilized. The resistivity meter on a laptop is connected to this gadget. A text file that can be read contains details on the measurement sequence, the kind of array utilized, and other survey components, such as the current intensity. The measurements are automatically saved to the laptop. By employing multi-core cables with 16 electrodes, the field data were used to build a pseudosection. The distance between adjacent electrodes is taken into account for the initial measurements in this investigation. Using electrodes 13, 14, 15, and 16, this procedure is repeated until the last measurement with spacing a is obtained. For spacing a, there were a total of 13 initial sequence readings. Using the following formula

$$\rho_a = 2\pi a \Delta V / I \ldots\ldots\ldots\ldots (2)$$

It is determined what the apparent resistivity a, for spacing a, is. where I is the produced current and V is the potential difference between the potential electrodes. Following the completion of the first sequence of measurements with spacing a, the second sequence of measurements with spacing 2a was made. The electrodes used for the initial measurement are 1, 3, 5 and 7.

Each pair of adjacent electrodes has a 2a gap between them thanks to careful electrode selection. The second measurement makes use of electrodes 2, 4, 6, and 8. In this procedure, electrodes 10, 12, 14, and 16 are employed up to the last measurement with spacing 2a. The process is repeated for measurements with the spacing of 3a, 4a, and 5. For spacing 5a, there is simply one measurement. As a result, when multi-core cables with 16 electrodes are laid once, there are 35 measurements altogether as opposed to just one for a conventional survey with four electrodes. As the electrode spacing expands, the number of measurements decreases.

2.8. Groundwater sampling and analyses

In order to collect water samples for hydrochemical studies, two plastic bottles that had been completely washed with distilled water were used at 49 sampling locations. One of the two sample bottles had strong nitric acid inside as a preservative. Nitric acid lowers the pH of water when it is dissolved in it, preventing precipitation of cations during transit. The groundwater obtained from the sampled borehole water was used to rinse the sample vials at least three

more times. All sample collection, labeling, sealing, and storage procedures were carried out in accordance with APHA (2011) guidelines. After the borehole's water was pumped for at least 10 minutes, all of the water samples were collected (Ketata et al. 2011). Since these values vary with ambient conditions, such as temperature, in situ measurements of physico-chemical parameters (EC, pH, TDS, and temperature) were conducted using the Hanna Instruments, USA, HI98130 model Combo Electrical Conductivity (EC) and pH meter. The GPSMap 76C global position system model was utilized to determine the geographic coordinates of the water sampling and VES locations, which were used to publish borehole and VES points on the geologic map (Fig. 1).Na^+ and K^+ concentrations were measured using a flame photometer, whereas total hardness ($CaCO_3$), calcium (Ca^{2+}), carbonate (CO_3^{2-}), bicarbonate (HCO_3^-), and chloride analyses were performed using a volumetric approach (Cl-). Sawyer et al. (2003) computed Mg2+ as follows from concentrations of total hardness and calcium:

$$Total\ Hardness\ \left(\frac{mg}{l}\right) = (Ca2^+ + Mg2^+)x\ 50\ \ldots\ldots\ldots\ldots\ldots\ldots\ldots\ldots\ldots\ldots (3)$$

Where the amounts of Ca2+ and Mg2+ are given in mg/l. The colorimetric method was used to measure sulfates (SO_4^{-3}) in the environment. The samples intended for heavy metal analysis were acidified with nitric acid to a pH of 2.

The concentrations of various anions, including nitrite (NO_2^-), nitrate (NO_3^-), phosphate (PO_4^{3-}), sulphate (SO_4^{2-}), and cations, including total iron (Fe), zinc (Zn), and manganese (Mn), were measured using the WAGTECH spectrophotometer method (Mn). All water samples were analyzed in the CRS-RUWATSSA Laboratory, Calabar, in accordance with the guidelines outlined by APHA (1995). The levels that were observed were compared to the drinking water guidelines set by the World Health Organization in 2010. During sample analysis, routine analyses of duplicates, blanks, and ionic balance checks were carried out. Cation-anion balance error was computed to satisfy the electroneutrality criteria and was found to be within 5%. (Osang et al 2020)

2.9. Household & Health surveys

At least 10 consecutive users of each of the 49 boreholes where samples were taken were questioned about their use of home water. Through a structured interview, trained student volunteers questioned respondents about their usage of the source for drinking, their knowledge of diseases transmitted through contaminated water, how they felt the water tasted, and why they chose it over other sources. The users' ages, health status, and the hospital or medical facilities they attend while ill were also inquired about. Interview questions were asked in their regional languages, and responses were recorded in English.

A section of the survey instrument was created to gather information about the respondents' health status; as a result, the questionnaire was given to the respondents at their preferred healthcare facility. Medical or health professionals served as guides as the respondents filled out the questionnaires. The nature of the study, the fact that participation was entirely voluntary, the fact that no personally identifying information would be included in the study report, and the fact that he or she could refuse to answer any question were all explained to the respondent prior to the start of each survey. Before the interviews began, the respondents verbally agreed. A total of 550 families, including 3600 people's health records, were covered. The research team conducted their work in compliance with all scientific norms, and standards of ethics as required by the health ministry and the Cross River University of Technology.

3. Results and discussion

3.1. Geoelectrical interpretation

Subsurface model generated from the VES data with constraints from lithologic logs were used to construct electrostratgraphic units Fig.2 shows samples of the modelled curves generated in the area.

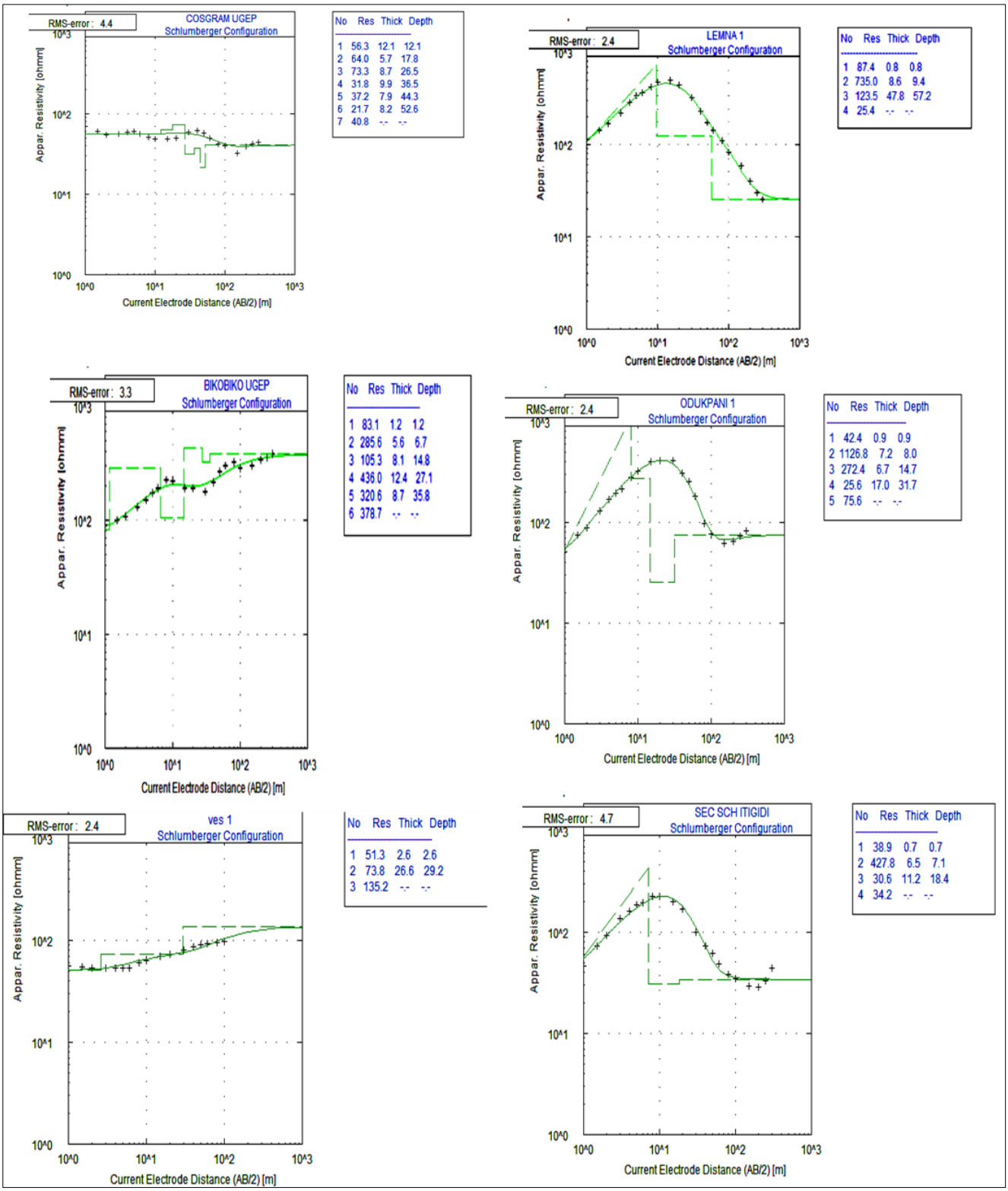

Figure 2 Sampled 1-D Inverted Resistivity Curve Models

These 1-D model curves were used to construct the geosection that reveals the subsurface stratigraphic distribution from northeast to southwest. The segment matched the lithologic description in the borehole log. (Fig. 3). The same geometric plane was thought to be shared by the distances between adjacent resistivity sounding points, lithologic logs, and 1-D inversion resistivity curves used to construct electrostratigraphic units. Based on the local geology, three significant sedimentary formations were identified: ARG, EAG, and NSG. In the epithelium electrostratigraphic unit, fine-textured argillaceous sediments with resistivity readings ≤ 200Ωm are the majority. These sediments, which have a

relatively low resistivity, cover the entire area from east to west. Directly below these very low-resistivity layers is a thin (3-7 m) unit with slightly higher resistivities that conforms to sandstone (>500Ωm) materials in the lithologic section. The lithologic log from the area of the research region known as Obubra shows the vertical and lateral continuities of the unit across the profile. This sandstone unit grades into a shaly deposit and is continuous with the Late Turonian-Coniacian calcareous Amaseri Sandstone ridge throughout the bulk of the study area (Odigi and Amajor 2009; Uquetan et al 2016). Underneath this thin (3.9-5.7 m) sandstone block, which is marked by higher resistivities (≥200Ωm), is an imbricate sand-shale unit that grades into clay in the areas around Ofombongha and Adun Beach At depths of about 25 meters, a sandstone pinch out that appears to be a component of the Turonian-Coniacian sandstone ridge was discovered.

Figure 3 Model showing Northwest – Southwest Geoelectric Psuedosection of the study area

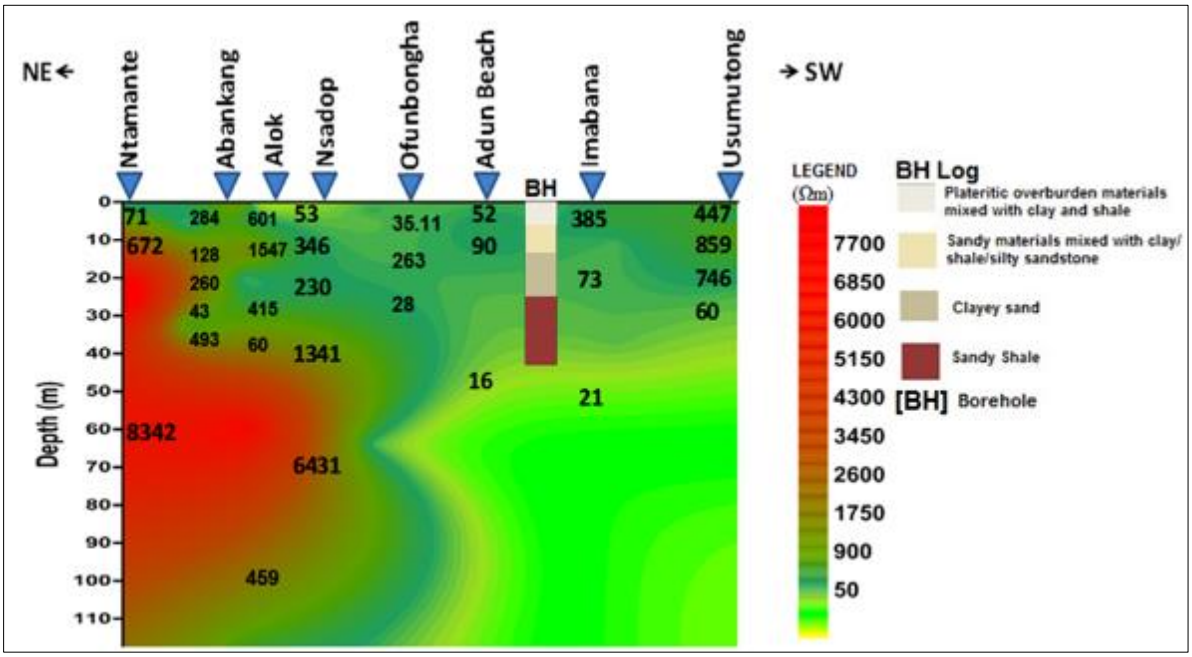

Source: Author's field work, (2022).

Figure 3 Sampled Geosection N-S Geosection

Towards the western end of the profile. Although its productivity is restricted by its lateral and vertical continuities, this structure is typically targeted during groundwater exploitation in the region. According to Akpan et al. (2013) and Petters (1989), this sandy horizon offers a moderate groundwater output and is the predominant source of drinkable water in the region. The area's aquifer unit is made up of a heavily fractured shale deposit that grades into the sandy-shale unit (Ebong et al. 2014; Uquetan et al 2016). The silty layer, which lies just beneath the fractured shale layer, is a target for groundwater exploitation. Four separate geoelectric strata were seen in the electrostratigraphic cross section (Fig. 5), which crosses the NSG and the EAG. The first layer's resistivities (148–1881 m) were understood to represent a thin (4-6 m) layer of sandy soils with various moisture and texture components. The second layer, which is made up of cemented sandstones and sands, has a resistivity range of 204 to 746 m and a thickness of 34 m. This layer is infrequently interrupted by the EAG's fractured shale (P>60 m) and a few intercalated clay layers (60 m). The fourth layer is covered by an impermeable layer that is made up of thick (about 8 m) shales. The impervious shale unit is underlain by the fourth layer, which is characterized by fine-medium-grained sandstone (saturated) and has moderate resistivity (121-364 m) values and thicknesses (5.5–12.0 m). In the southern part of the research area, this layer makes up the aquifer horizon. The aquifer horizons are anisotropic and inhomogeneous, especially in the northern region. Variations in geography, the aquifer horizon's textural composition, and tectonic history all have a significant impact on the directions that groundwater flows. Groundwater table depths during the dry season often range between 25 and 40 m, depending on local paleo-tectonic disturbances. These disruptions caused secondary aquifer features to emerge, such as fractures and joints, as well as the deformation of sandstones, shalestones, and shally sediments. These changes also improved groundwater conveyance and yield (Okereke et al. 1998; Raju and Reddy 1998; Uquetan et al 2016). Additionally, seasonal variables have a significant impact on water table levels. For example, during wet seasons, groundwater tables are often high (3-5 m in low-lying areas and 10-20 m elsewhere) as a result of an increase in water

levels inside the Cross River that causes a direct inflow of river water landwards. Table 1 lists the lithologic and shallow subsurface resistivity variations in the research area.

Table 1 Summary of resistivity ranges and lithologic description

Resistivity (Ohm-m)	Lithologic Description
>50	Clay
50-100	Silt/Shale
100-250	Fine sand
250-450	Fine-to-medium sand
450-750	Medium-to-coarse sand
750-950	Consolidated Sand
>950	Dry unconsolidated sand

3.2. ERT RESULTS

The collected ERT data was examined using RES2DINV. A 5.00m cell width model was used to provide sharp images of the subsurface resistivity structure since the findings of the inversion model show significant fluctuations in the apparent resistivity (a). The resistivity tomograms are inverted, as seen in Fig. 4 below (a & b)

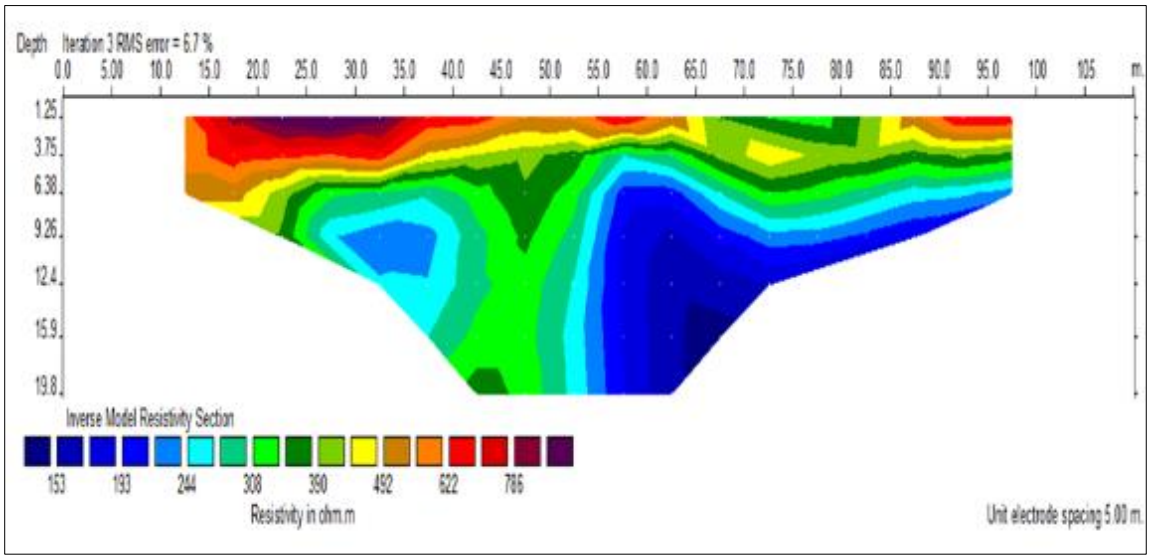

Figure 4a Sampled Inverted Resistivity Tomograms

In Fig. 4a, Five resistivity zones were delineated in the profile in the subsurface at different surface points the low resistivity zone (deep blue), with lowest resistivity < 200 Ωm is isolated at surface point 26-37m and 54-96m at depth of 7.0 - 11.0m and 6.0 - 19.8m, zone of highest resistivity <786Ωm isolated at surface point of 17.8 -35m and depth of 1.2m to3.2.0m. there is also a moderately low resistivity zone of <280Ωm (light blue) occurred at surface points between 25.0m to 40.0m and 51.0m to 95.5m at depths between 7.0m -13.1m and 5.0 to 19.5m, there is also a moderately high resistivity zone (red) with resistivity of <622Ωm, spread around two-third of the profile and occurring at surface point of 11.8m to 63.0m and 86.0 to 96.0m and 58.6m at depth of 1.25-5.8m. The zone with intermediate resistivity values (deep green) of <390Ωm occurred at surface points of 15.0m to 98.0m at depth of 1.25m to 19.8m. There is this general observation that, arising from the tomograms and the resistivity values realized from the area surveyed, the area is formidable enough not to allow contaminant infiltration through the subsurface.

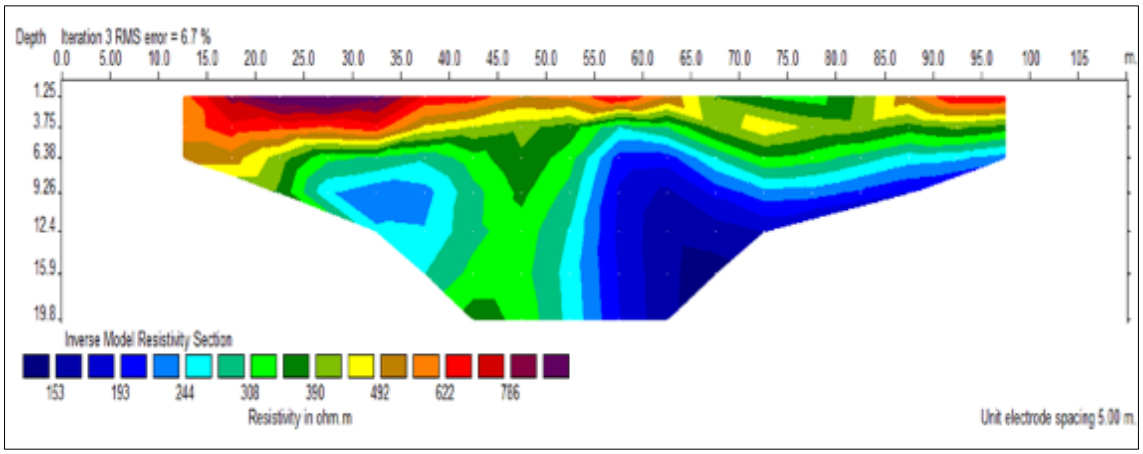

Figure 4b Sampled Inverted Resistivity Tomograms

Fig 4b show four resistivity zones, the lowest resistivity zone (deep blue) <120Ωm isolated at surface points between 16m and 34m of at a depth of 1.25m to 5.8m. there is also a zone of moderately low resistivity (light blue) with respectively of <136Ωm, isolated at surface points between 15.0m and 35.0m occurring a depth of 1.250m to 7.0m. The intermediate resistivity zone (deep green) has values of <280Ωm, occurred at surface points 13.0 – 15.0m, 35.0-38.0m,38.0-40.0m and 60.0m to 72.0m at a depth of 1.25m and 15.0m. The zone with the second to the highest resistivity value (red) of <600Ωm occurred at surface points of 42.0m to 45.0m and 64.0m to 72.0m at a depth of 1.25m to 15.9m. The zone with the highest resistivity (deep black) of >833Ωm occurred at surface point 45.0m and 65.0m and 72.0-78.0m at depth between 1.25 - 12.40.

3.3. Hydrochemistry and water quality

As groundwater flows within porous and permeable media, its chemical composition is determined by the soluble components of the rocks and soils it comes into contact with (Ragunath 1987 ; Uquetan et al 2016). Potential sources of cation and anion concentrations in the groundwater system include the lithologic makeup of the vadose zone materials and the rock chemistry of groundwater conduits. More so, they might be caused by humans, such as through seepages of industrial wastewater, municipal waste, untreated sanitary facilities, or chemicals in soil that, if not attenuated during the leaching process, will negatively impact the physical, chemical, and biological properties of the groundwater system (Sakthimurugan 1995)The correlation coefficients of the ions in the groundwater samples were determined using Pearson's correlation matrix, a bivariate method typically used in geological research to demonstrate how well one variable may predict the other. The cations and the anions developed separate sets of robust connections (Table 3). The data were adjusted to have values between 0.1 and 0.9 before to the creation of the correlation matrix using the following equation

$$X_n = 0.8 \times \left\{ \frac{x_i^n - x_{min}}{x_{max} - x_{min}} \right\} + 0.1 \quad \ldots\ldots\ldots\ldots\ldots\ldots\ldots\ldots\ldots\ldots\ldots\ldots\ldots\ldots\ldots (4)$$

Where X max and X min are the maximum and minimum values, respectively, and Xn is the normalized value, Xi is the measured value. It was thought that normalization (scaling) was necessary to prevent saturation from occurring when higher values predominated over lower ones. Additionally, scaling results in values losing their dimension (Ozcep et al. 2010). Depending on the statistical significance of the calculated correlation, the level of links found in the Pearson correlation matrix ranges from -1 to +1. (Ketata et al. 2011). Strong correlation was defined as a correlation coefficient >0.7, while moderate correlation was defined as a correlation coefficient between 0.5 and 0.7. (Giridharan et al. 2008). Negative coefficients showed that the variables under consideration were moving in opposite directions. The correlation coefficients of the highly competitive ions were found to be weak based on the Douglas and Leo (1977) groundwater chemistry correlations, such as Na+ with Mg+ (-0.11), Ca^+ with Na^+ (-0.18), and SO_4^{2-} with Cl^- (-0.60). Ca^+ and SO_4^{2-} have a strong affinity ion interaction (0.81), however other ions such as Na^+ and Cl^- and Mg^{2+} and SO_4^{2-} and Na^+ and HCO_3^- and K^+ and HCO_3^- have weak relationships. With the exception of HCO_3^- and Cl^-, the non-competitive interactions were likewise weakly connected (-0.60).

The most popular graphical tool for evaluating geochemical data is the Piper diagram (Piper 1944). According to the design, which showed two distinct trilinear plots flanking a diamond-shaped central plot, the relative concentrations of main cations and anions in water samples can be assessed (Guler et al. 2002; Uquetan et al 2017). The graphic

represents the overall chemical properties of the sampled water, which are a result of the evolutionary paths (Freeze and Cherry 1979) or a mixture of groundwater and weathered components from host formations (Ragunath 1987). Water samples with comparable characteristics will typically plot as groups (Todd and Mays 2005).The results of 49 samples of borehole water compositions in the region shown on the Piper diagram are shown in Fig. 5. The clusters serve as markers of the local water type. The Ca-Mg-CO_3-HCO_3 concentration was clearly dominant in the water facies, according to the Piper plot. According to Handa (1979), such water facies suggest an adequate recharge from a freshwater aquifer and water with transitory hardness. The geosection of the research area's material composition reveals that alkaline earth metals, such as Ca^{2+} and Mg^{2+}, outnumber alkalis, such as Na^{+} and K^{+}. Reduced K^{+} in groundwater results from clay mineral fixation, which causes nutrient loss and weather resistance (Kolahchi and Jalali 2006). Strong acids, such as Cl^{-} and SO_2, are outweighed by weak acids, such as HCO_3^{-}, demonstrating the superiority of alkaline earth metals over bicarbonates (Subba Rao 2002). This suggests that Na^{+} and alkaline earth metals are traded, resulting in base exchanged toughened water. This finding is consistent with the groundwater reports of Akpan et al. (2013) for the Ikom Mamfe Embayment. The range of groundwater temperatures is 26 to 29 ^{0}C. (Average of 27.5 ^{0}C). The WHO (2010) acceptable maximum of 30 ^{0}C for drinking water is met by these values. The groundwater's pH, or proton acidity, ranges from 4.9 to 8.4, with an average of 6.56. (Table 3 a & b). Acidic groundwater samples have a pH below 6.5, which shows that there are less hydroxide ions there than there are hydrogen ions, which are found in plenty. 62% of the water sampled was alkaline (pH 6.5), compared to 38% of the acidic water (pH 6.5). Acidic groundwater may be caused by human activity and careless sewage disposal in certain areas. The increased water acidity could potentially be caused by weathering processes within aquifer horizons. Values of groundwater electrical conductivity (EC) which is a measure of the ease, in which water conducts electric current range from 64.70 to 182.00 µS/cm at 25 ^{0}C. These observations are below WHO (2010) tolerable limit of 1400 µS/cm for drinking and agricultural water needs. EC values approximately capture the total amount of dissolved substances in water. It depends on temperature, concentration, and type of ions present (Hem 1989; Uquetan et al 2017).

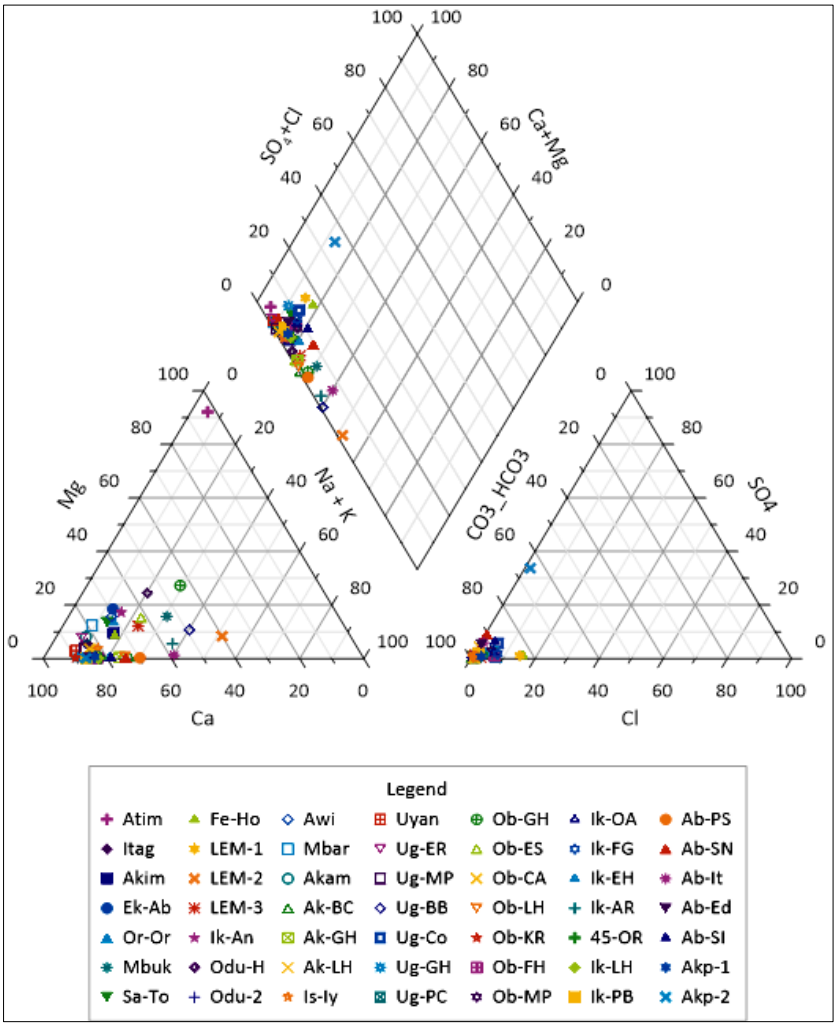

Figure 5 Piper Diagram for Groundwater Investigation in some Urban Communities in Cross River State

Table 3a Results of Physiochemical Parameters

NAME	STATION	PH	NO2(mg/L)	Electrical Conductivity (ps/cm)	TDS (mg/L)	BOD (mg/L)	DO (mg/L)	Sulphate (mg/L)	Zinc (mg/L)	ARSENIC	TSS (mg/L)	Alluminium (mg/L)	Barium (mg/L)	Chromium (mg/L)	Cadium (mg/L)	Copper (mg/L)	Cynides (mg/L)	Flouride (mg/L)	Iron (mg/L)	Lead (mg/L)	Magnessium (mg/L)
NAME	STATION	pH	NO2	EC	TDS	BOD	DO	SO4	Zn	As	TSS	Al	Ba	Cr	Cd	Cu	CN-	F	Fe	Pb	Mg
Atimbo	Atim	6.10	0.10	81.50	24.10	1.60	1.40	2.45	0.22	BDL	0.00	0.02	0.03	0.05	0.02	0.01	0.01	0.13	0.01	0.03	40.00
Itagbo	Itag	6.50	0.40	105.50	31.20	1.80	1.00	2.15	0.21	BDL	ND	0.06	0.02	0.01	0.04	0.01	ND	0.12	0.02	0.04	2.00
Akim	Akim	6.00	0.10	100.00	20.10	2.10	1.80	2.66	0.19	BDL	ND	0.01	0.01	0.04	0.02	0.01	0.01	0.90	0.01	0.01	2.00
Ekpo Abasi	Ek-Ab	5.00	0.04	102.40	21.40	3.20	2.00	2.10	0.18	BDL	0.00	0.08	0.01	0.02	0.01	0.01	ND	0.80	0.03	0.03	3.00
Orok Orok	Or-Or	6.80	0.10	108.50	15.40	4.60	1.90	1.77	0.20	BDL	0.00	0.04	0.01	0.03	0.02	0.02	0.01	1.00	0.01	0.02	5.00
Mbukpa	Mbuk	8.20	0.06	111.00	16.80	1.80	2.10	3.10	0.19	BDL	0.00	0.01	0.02	0.01	0.05	0.02	0.01	0.80	0.04	0.01	4.00
Satellite Town	Sa-To	7.60	0.05	120.50	31.20	1.50	1.20	2.40	0.30	0.05	0.00	0.01	0.01	0.05	0.01	0.01	0.01	0.90	0.05	0.04	3.00
Federal Housing	Fe-Ho	6.80	0.09	89.40	38.50	1.90	1.30	2.10	0.20	BDL	ND	0.02	0.01	0.02	0.03	0.02	0.01	0.60	0.03	0.03	2.00
LEMNA I	LEM-1	5.80	0.10	120.00	150.10	7.00	1.40	2.20	0.16	BDL	ND	0.01	0.02	0.03	0.05	0.01	ND	0.80	0.01	0.02	1.00
LEMNA II	LEM-2	5.60	0.10	150.00	120.10	1.50	1.90	1.90	0.08	BDL	ND	0.03	0.02	0.02	0.01	0.02	0.01	0.70	0.02	0.05	1.00
LEMNA III	LEM-3	6.10	0.09	160.50	110.10	6.10	2.50	1.80	0.15	BDL	ND	0.07	0.01	0.04	0.02	0.02	0.00	0.70	0.02	0.02	2.00
Ikot Ansa	Ik-An	5.20	0.10	96.10	10.60	1.90	1.60	1.99	0.18	BDL	ND	0.05	0.00	0.05	0.01	0.02	0.00	0.06	0.01	0.03	4.00
Odukpani Hqtrs	Odu-H	6.10	0.09	89.60	20.60	1.50	1.50	1.84	0.24	BDL	ND	0.04	0.01	0.01	0.02	0.02	ND	0.60	0.04	0.06	5.00
Odukpani II	Odu-2	6.20	0.10	78.10	25.60	6.10	1.30	1.40	0.22	BDL	ND	0.01	0.01	0.01	0.03	0.09	0.01	0.80	0.05	0.01	0.8
Awi	Awi	6.50	0.08	64.70	21.60	2.10	1.40	1.13	0.16	BDL	ND	0.02	0.02	0.02	0.05	0.01	0.01	0.01	0.01	0.02	4
Mbarakom	Mbar	6.70	0.09	89.10	19.00	2.80	1.60	2.11	0.08	BDL	ND	0.03	0.02	0.03	0.04	0.09	0.00	0.80	0.02	0.03	3
Akamkpa	Akam	6.00	0.01	101.50	18.10	1.50	2.10	2.00	0.15	BDL	ND	0.04	0.01	0.02	0.01	0.02	0.01	0.90	0.03	0.09	2
Akamkpa base camp	Ak-BC	7.0	0.2	130.0	7.2	2.0	1.9	1.8	0.4	ND	1.00	10.00	0.90	0.02	0.00	0.07	0.00	0.90	0.09	0.02	0.12
Akamkpa General Hospital	Ak-GH	5.9	0.3	150.0	15.1	1.6	2.1	1.9	0.1	ND	0.80	0.09	0.80	0.08	0.00	0.10	0.00	0.66	0.10	0.01	0.1
Akamkpa LGA Hqtrs	Ak-LH	6.2	0.4	180.0	11.5	1.7	1.2	6.0	0.8	ND	2.00	0.02	1.60	0.06	0.00	0.50	0.00	0.64	0.20	0.00	0.09
Isong Iyang	Is-Iy	5.80	0.06	106.10	21.50	1.90	2.50	3.00	0.09	BDL	ND	0.01	0.01	0.02	0.08	0.02	0.01	1.00	0.02	0.01	1

Uyangha	Uyan	4.90	0.07	126.10	16.50	3.40	2.60	2.40	0.10	BDL	ND	0.03	0.01	0.04	0.02	0.01	ND	1.20	0.02	0.02	1
Ugep Ediba Road	Ug-ER	6.50	0.10	111.50	0.80	1.80	2.50	1.62	0.10	BDL	ND	0.04	0.19	0.08	0.05	0.01	ND	0.90	0.01	0.02	2
Ugep Motor Park	Ug-MP	6.10	0.09	180.10	0.90	1.60	1.40	1.24	0.07	BDL	ND	0.01	0.02	0.03	0.06	0.02	ND	0.80	0.04	0.04	1
Ugep Biko Biko	Ug-BB	6.20	0.05	182.30	10.10	1.90	1.80	1.31	0.13	BDL	ND	0.02	0.02	0.01	0.04	0.01	0.01	0.90	0.03	0.00	1
Cosgram Ugep	Ug-Co	6.2	0.3	106.5	81.1	1.1	1.3	12.1	0.7	ND	1.05	0.09	0.75	0.02	0.01	0.80	0.01	0.90	0.03	0.01	0.07
Gen. Hospital Ugep	Ug-GH	6.1	0.1	118.2	8.1	1.5	1.8	6.4	1.0	ND	0.80	0.01	0.10	0.03	0.00	0.40	0.01	0.80	0.02	0.01	0.08
PCN Ugep	Ug-PC	7.2	0.1	124.0	21.6	3.1	2.1	3.1	0.9	ND	0.95	0.02	1.20	0.05	0.00	0.09	0.01	1.02	0.08	0.01	0.1
Obubra Gen. Hospital	Ob-GH	6.80	0.10	134.00	6.20	1.80	0.40	1.10	0.12	BDL	ND	0.01	0.04	0.02	0.02	0.03	0.01	1.00	0.06	0.04	3
Obubra Excellence Sch.	Ob-ES	7.20	0.09	120.00	1.80	1.90	1.00	0.06	0.11	BDL	ND	0.01	0.01	0.03	0.03	0.04	ND	0.80	0.02	0.02	2
Obubra Chief Alex Road	Ob-CA	7.30	0.05	101.50	7.50	1.50	1.60	0.50	0.13	BDL	ND	0.01	0.01	0.01	0.04	0.08	0.01	0.90	0.01	0.03	0.8
Obubra LGA Hqtrs	Ob-LH	7.0	0.1	100.5	8.4	2.1	1.4	0.4	0.1	BDL	ND	0.01	0.01	0.01	0.05	0.02	0.01	0.80	0.04	0.05	0.1
Obubra Kwakwa Road	Ob-KR	5.8	0.1	88.5	10.5	1.2	1.9	6.2	0.6	BDL	0.00	0.09	0.90	0.01	0.00	0.10	0.01	0.90	0.02	0.01	0.09
Obubra Fedral Housing	Ob-FH	5.5	0.1	110.0	6.8	1.8	2.1	1.2	1.2	0.00	0.02	0.08	0.80	0.02	0.00	0.11	0.00	0.08	0.08	0.01	0.06
Obubra Motor Park	Ob-MP	6.1	0.1	112.0	76.1	0.9	2.9	3.4	1.0	0.01	0.08	0.09	1.00	0.01	0.00	0.09	0.01	1.00	0.04	0.01	0.05
#7 Okim Asabor Ikom	Ik-OA	6.8	0.1	77.6	17.1	5.1	1.5	1.9	0.2	BDL	0.00	0.01	0.01	0.01	0.03	0.01	0.01	0.18	0.03	0.04	0.02
Ikom Fed. Govt. College	Ik-FG	6.9	0.1	86.1	10.4	3.1	1.6	1.8	0.1	BDL	ND	0.02	0.02	0.04	0.01	0.02	0.01	0.50	0.04	0.02	0.08
Ikom Ekabokom Hill	Ik-EH	5.9	0.0	90.5	11.5	2.0	1.9	2.0	0.1	BDL	0.00	0.01	0.01	0.03	0.02	0.01	0.01	0.60	0.05	0.08	0.09

Ikom Agbokim Road	Ik-AR	5.8	0.3	95.5	10.8	2.1	2.0	1.8	0.1	BDL	0.00	0.02	0.01	0.01	0.02	0.00	ND	0.80	0.05	0.02	1
45 Obubra Road Ikom	45-OR	6.1	0.1	112.0	76.1	0.9	2.9	3.4	1.0	0.01	0.08	0.09	1.00	0.01	0.00	0.09	0.01	1.00	0.04	0.01	0.05
LGA Hqtrs Ikom	Ik-LH	7.1	0.1	120.5	50.1	1.6	3.1	1.8	0.7	0.01	1.00	0.01	0.90	0.04	0.00	0.02	0.01	0.08	0.50	0.01	0.009
Police Banned Ikom	Ik-PB	7.0	0.2	101.5	18.4	2.1	1.6	4.6	0.8	BDL	1.50	0.08	0.50	0.05	0.01	0.02	0.01	0.06	0.10	ND	0.02
Abi Police Station	Ab-PS	8.2	0.2	96.4	19.0	2.5	1.3	1.9	1.0	ND	0.04	0.05	0.40	0.01	0.00	0.01	0.01	0.81	0.90	0.00	0.04
Abi School of Nursing	Ab-SN	8.4	0.1	90.5	11.5	2.2	1.8	20.1	0.9	ND	0.01	0.02	0.50	0.08	0.00	0.03	0.01	0.46	0.10	0.01	0.05
Abi Itigidi	Ab-It	8.0	0.3	120.1	28.0	2.3	2.0	18.2	1.1	ND	0.80	0.01	0.09	0.06	0.01	0.05	0.00	0.18	0.15	0.01	0.1
Abi Ediba	Ab-Ed	7.9	0.2	114.0	24.1	2.4	1.3	15.3	1.5	ND	1.60	0.01	0.08	0.01	0.00	0.06	0.01	0.61	0.09	0.01	0.09
Abi Sec. Sch. Itigidi	Ab-SI	7.5	0.6	111	20	2.1	1.2	15.9	0.9	ND	3.40	0.07	0.40	0.03	0.01	0.01	0.01	0.55	0.05	0.00	0.06
Akpet I	Akp-1	6.9	0.0	106.1	12.1	6.4	1.4	2.0	0.2	BDL	ND	0.01	0.01	0.02	0.04	0.01	0.01	1.10	0.02	0.03	0.2
Akpet II	Akp-2	8.1	0.2	105.2	75.0	1.9	2.6	81.2	0.8	ND	1.55	0.01	0.60	0.01	0.08	0.15	0.01	1.00	0.04	0.00	0.05
Minimum		4.90	0.01	64.70	0.80	0.90	0.40	0.06	0.05	0.00	0.00	0.01	0.00	0.01	0.00	0.00	0.00	0.01	0.01	0.00	0.01
Maximum		8.40	0.60	182.30	150.10	7.00	3.10	81.20	1.50	0.05	3.40	10.00	1.60	0.08	0.08	0.80	0.01	1.20	0.90	0.09	40.00
Mean		6.56	0.13	111.77	28.37	2.42	1.77	5.32	0.41	0.02	0.64	0.24	0.27	0.03	0.02	0.07	0.01	0.69	0.07	0.02	2.01
SD		0.84	0.11	25.49	31.67	1.42	0.54	11.85	0.38	0.02	0.83	1.41	0.40	0.02	0.02	0.14	0.00	0.32	0.14	0.02	5.67
NSDWQ 2015		6.5-8.5	0.2	1000	500	10	5	100	3	0.01	500	0.2	1.3	0.05	0.003	1	0.01	1.5	0.3	0.01	0.2

Table 3b Results of Physiochemical Parameters

NAME	STATION	Mercury (mg/L)	Nickel (mg/L)	Nitrate (mg/L)	Total Hardness as CaCO3 (mg/L)	Residual Cl_2 (mg/L)	Sodium (mg/L)	Alkalinity	Ca	Salinity as NaCl(mg/L)	HCO3-	Cl	PO4	K	NH4	Mn	CO3	Colour	Odour	Taste	Turbidity (FTu)	Temperature (^{0}C)	FCC(100 ml/cfu)	TCC (100ml/ cfu)	APPARENT Resistivity (ohm-Metre)
NAME	STATION	Hg	Ni	NO_3-	CaCO3	Residual Cl2	Na	Alkalinity	Ca	NaCl	HCO3-	Cl	PO4	K	NH4	Mn	CO3	Colour	Odour	Taste	Turbidity	Temper	aFCC	TCC	App. Resistivity
Atimbo	Atim	ND	0.02	2.30	92.20	0.15	1.28	70.0	1.2	3.2	124.2	4.8	0.3	1.0	0.1	0.0	91.0	<5	Unobj	Unobj	0.17	28.50	0	0	17.8
Itagbo	Itag	ND	0.03	3.10	79.60	0.10	1.33	73.0	30.1	1.0	98.4	2.0	2.5	2.6	0.2	0.0	49.5	<5	Unobj	Unobj	0.11	29.00	0	0	75.2
Akim	Akim	ND	0.01	4.20	198.30	0.00	2.15	150.0	15.5	3.4	14.8	3.4	9.0	1,5	0.1	0.0	182.8	<5	Unobj	Unobj	0.12	28.50	0	0	49.4
Ekpo Abasi	Ek-Ab	ND	0.02	2.50	288.10	0.10	1.53	72.0	11.2	1.2	308.7	10.7	0.2	0.5	0.1	0.0	276.9	<5	Unobj	Unobj	0.10	28.00	0	0	230.5
Orok Orok	Or-Or	ND	0.02	3.30	162.30	0.11	2.76	ND	25.1	6.9	350.6	40.8	2.1	2.4	0.3	0.0	137.2	<5	Unobj	Unobj	0.20	29.00	0	0	154.2
Mbukpa	Mbuk	ND	0.01	4.50	78.90	0.11	2.30	70.0	13.6	4.2	120,7	9.9	0.1	5.5	0.2	0.0	65.3	<5	Unobj	Unobj	0.19	28.00	0	0	210.7
Satellite Town	Sa-To	ND	0.08	2.20	70.20	0.16	1.08	16.0	16.1	3.8	121.7	13.5	2.9	1.8	0.3	0.0	54.1	<5	0.01	0.01	0.11	29.00	0	0	212
Federal Housing	Fe-Ho	ND	0.06	2.70	66.80	0.15	2.05	20.6	17.2	0.8	132.4	34.7	1.9	2.2	0.2	0.0	49.6	<5	Unobj	Unobj	0.14	29.00	0	0	410
LEMNA I	LEM-1	ND	0.09	2.50	78.60	0.20	1.73	15.0	24.1	0.5	122.6	31.0	1.1	2.5	0.1	0.0	54.5	<5	Unobj	Unobj	0.16	28.00	4	10	123.9
LEMNA II	LEM-2	ND	0.02	2.10	54.10	0.18	1.10	24.0	4.8	4.0	92.4	0.6	1.4	5.1	0.1	0.0	49.3	<5	Unobj	Unobj	0.13	29.00	0	0	180.6
LEMNA III	LEM-3	ND	0.02	4.30	101.10	0.14	2.68	21.0	10.6	4.9	311.9	12.1	1.9	1.2	0.2	0.0	90.5	<5	Unobj	Unobj	0.11	28.50	1	8	167.3
Ikot Ansa	Ik-An	ND	0.16	2.80	389.10	0.15	1.36	32.0	15.6	4.0	210.9	10.0	1.0	2.3	0.1	0.0	373.5	<5	Unobj	Unobj	0.10	28.00	0	0	56.1
Odukpani Hqtrs	Odu-H	ND	0.24	1.90	78.70	0.13	2.33	70.0	11.3	3.6	97.8	0.9	1.0	1.8	0.2	0.0	67.4	<5	Unobj	Unobj	0.10	29.00	0	0	46.2
Odukpani II	Odu-2	ND	0.12	1.80	211.50	ND	1.19	56.0	15.1	3.2	39.9	1.9	2.5	1.0	0.1	0.0	196.4	<5	Unobj	Unobj	0.20	29.00	0	0	70.1
Awi	Awi	ND	0.18	2.00	96.30	0.15	1.06	51.1	18.1	4.5	210.9	8.0	1.5	2.4	0.1	0.0	78.2	<5	Unobj	Unobj	0.20	28.50	0	0	412.1
Mbarakom	Mbar	ND	0.01	2.10	121.20	0.10	1.00	50.0	19.1	2.1	160.9	1.4	2.1	1.2	0.2	0.0	102.1	<5	Unobj	Unobj	0.90	29.00	0	0	112.1
Akamkpa	Akam	ND	0.05	2.40	66.70	0.20	1.23	61.0	20.2	3.1	123.1	0.9	8.6	1.0	0.1	0.0	46.5	<5	Unobj	Unobj	1.30	29.00	0	0	70.1
Akamkpa base camp	Ak-BC	ND	0.01	1.79	123.00	1.30	3.10	0.8	13.4	2.0	300.1	0.1	4.8	1.8	0.2	0.0	109.6	<5	Unobj	Unobj	4.0	28.5	0	0	411.8
Akamkpa General Hospital	Ak-GH	ND	0.01	2.29	93.00	0.98	3.00	0.8	16.1	5.8	157,4	1.8	5.8	2.0	0.1	0.0	76.9	<5	Unobj	Unobj	3.0	28.5	0	0	253.1
Akamkpa LGA Hqtrs	Ak-LH	ND	0.02	2.50		0.79	1.87	1.0	18.1	3.5	154.6	1.1	2.2	1.2	0.2	0.0	-18.1	<5	Unobj	Unobj	4.0	29.0	0	0	73.5
Isong Iyang	Is-Iy	ND	0.06	1.85	189.30	0.10	0.92	71.0	22.1	2.3	150.1	1.9	1.4	3.2	0.3	0.0	167.2	<5	Unobj	Unobj	1.10	28.50	0	0	31.3
Uyangha	Uyan	ND	0.08	1.60	176.00	0.11	1.02	70.1	29.6	4.1	132.9	2.9	1.4	1.9	0.2	0.0	146.4	<5	Unobj	Unobj	0.90	29.00	0	0	415
Ugep Ediba Road	Ug-ER	ND	0.02	5.20	96.00	0.16	1.24	56.5	21.8	2.1	130.8	2.0	1.6	0.9	0.3	0.0	74.2	<5	Unobj	Unobj	1.10	29.50	0	0	150
Ugep Motor Park	Ug-MP	ND	0.07	5.10	210.10	0.15	2.16	55.0	21.1	5.8	125.6	1.7	1.9	0.6	0.2	0.0	189.0	<5	Unobj	Unobj	0.90	29.50	0	0	143.9
Ugep Biko Biko	Ug-BB	ND	0.07	5.80	171.10	0.11	2.06	52.0	4.6	4.5	140.7	0.9	1.6	1.7	0.2	0.0	166.5	<5	Unobj	Unobj	0.70	28.00	0	0	101.7
Cosgram Ugep	Ug-Co	ND	0.02	2.21	82.10	0.80	1.60	1.0	15.6	7.0	122.9	12.4	0.1	1.1	0.2	0.0	66.5	<5	Unobj	Unobj	6.0	28.5	0	0	2162.1

Gen. Hospital Ugep	Ug-GH	ND	0.03	2.10	94.50	0.96	0.99	0.9	18.4	2.1	98.9	11.0	0.2	1.2	0.1	0.0	76.1	<5	Unobj	Unobj	2.0	28.6	0	0	46.1
PCN Ugep	Ug-PC	ND	0.01	1.82	75.30	0.76	2.46	1.0	19.1	6.0	89.6	8.9	7.8	1.2	0.2	0.0	56.2	<5	Unobj	Unobj	5.0	29.0	0	0	500.1
Obubra Gen. Hospital	Ob-GH	ND	0.02	2.90	123.40	0.20	1.80	50.0	4.8	3.1	101.6	4.9	6.4	1.4	0.1	0.0	118.6	<5	Unobj	Unobj	1.00	29.00	0	0	180.4
Obubra Excellence Sch.	Ob-ES	ND	0.01	2.40	151.10	0.15	1.90	54.0	8.1	2.9	201.9	3.2	5.3	1.1	0.1	0.0	143.0	<5	Unobj	Unobj	0.80	28.50	0	0	98.4
Obubra Chief Alex Road	Ob-CA	ND	0.01	2.10	161.20	0.20	1.58	17.6	18.4	0.9	209.9	3.9	5.0	1.2	0.1	0.0	142.8	<5	Unobj	Unobj	0.80	28.50	0	0	139.7
Obubra LGA Hqtrs	Ob-LH	ND	0.02	2.40	112.20	0.19	1.66	21.0	10.5	1.1	176.4	1.9	2.9	1.9	0.3	0.0	101.7	<5	Unobj	Unobj	2.0	29.0	0	0	142.6
Obubra Kwakwa Road	Ob-KR	ND	0.02	1.50	50.50	0.15	1.24	0.9	30.1	1.7	211.1	2.1	3.8	2.1	0.1	0.0	20.4	<5	Unobj	Unobj	6.0	28.5	1	0	427.3
Obubra Fedral Housing	Ob-FH	0.0001	0.01	1.80	74.30	0.95	1.35	0.8	31.5	3.9	98.9	11.0	1.2	5.0	0.1	0.0	42.8	<5	Unobj	Unobj	5.0	28.1	0	0	223.9
Obubra Motor Park	Ob-MP	ND	0.01	2.00	81.40	0.50	2.40	1.0	18.6	1.9	49.9	5.9	1.1	1.6	0.1	0.0	62.8	<5	Unobj	Unobj	7.0	29.0	0	0	316.8
#7 Okim Asabor Ikom	Ik-OA	ND	0.08	2.00	18.20	0.14	0.90	20.0	14.1	5.3	70.9	4.9	2.4	1.9	0.2	0.0	4.1	<5	Unobj	Unobj	1.0	28.0	0	0	68.1
Ikom Fed. Govt. College	Ik-FG	ND	0.09	1.90	20.80	0.15	1.60	24.0	15.8	4.7	89.6	7.8	2.9	1.4	0.1	0.0	5.0	<5	Unobj	Unobj	0.8	29.0	0	0	452
Ikom Ekabokom Hill	Ik-EH	ND	0.05	1.80	22.30	0.20	1.90	21.6	19.6	3.1	79.8	2.9	4.2	3.2	0.1	0.0	2.7	<5	Unobj	Unobj	0.3	29.5	0	0	116.3
Ikom Agbokim Road	Ik-AR	ND	0.06	1.90	26.40	0.18	1.70	16.0	10.3	1.6	97.8	1.0	1.0	5.1	0.2	0.0	16.1	<5	Unobj	Unobj	0.6	29.5	0	0	231.8
45 Obubra Road Ikom	45-OR	ND	0.01	2.00	81.40	0.50	2.40	1.0	18.6	1.8	120.9	4.9	6.4	1.6	0.3	0.0	62.8	<5	Unobj	Unobj	7.0	29.0	0	0	316.8
LGA Hqtrs Ikom	Ik-LH	ND	0.00	1.90	70.80	1.00	1.84	1.0	19.4	0.9	125.6	5.1	3.5	2.2	0.3	0.0	51.4	<5	Unobj	Unobj	3.0	29.0	1	2	49.5
Police Banned Ikom	Ik-PB	ND	0.01	1.40	100.00	1.05	1.06	0.0	20.5	0.5	132.4	3.2	2.1	2.1	0.1	0.0	79.5	<5	Unobj	Unobj	4.0	30.0	0	0	98.9
Abi Police Station	Ab-PS	ND	0.01	0.95	97.30	0.90	1.85	150.0	11.5	4.9	143.8	2.0	6.2	3.1	0.2	0.0	85.8	<5	Unobj	Unobj	6.0	29.0	0	0	500.9
Abi School of Nursing	Ab-SN	ND	0.02	0.82	91.40	0.80	2.10	120.0	11.6	7.0	118.7	0.9	0.1	1.9	0.1	0.0	79.8	<5	Unobj	Unobj	3.0	28.0	0	0	46.8
Abi Itigidi	Ab-It	0.0001	0.01	0.99	93.50	0.16	2.00	148.0	4.8	1.2	197.0	3.2	2.4	1.3	0.2	0.0	88.7	<5	Unobj	Unobj	4.0	28.5	0	0	3197.1
Abi Ediba	Ab-Ed	ND	0.01	0.89	90.50	0.12	1.90	1.2	20.1	2.9	201.6	1.9	1.1	1.3	0.1	0.0	70.4	<5	Unobj	Unobj	5.0	29.0	0	0	38.2
Abi Sec. Sch. Itigidi	Ab-SI	ND	0.01	1.84	89.00	0.51	1.56	1.8	23.1	0.2	160.5	11.2	3.2	4.6	0.1	0.0	65.9	<5	Unobj	Unobj	5	29.5	0	1	70.1
Akpet I	Akp-1	ND	0.09	1.90	160.00	0.16	2.01	30.0	25.6	4.6	130.7	8.1	1.1	2.8	0.1	0.0	134.4	<5	Unobj	Unobj	2.0	28.0	0	0	62.4
Akpet II	Akp-2	ND	0.01	1.69	71.10	0.58	1.55	130.0	22.6	2.2	106.6	4.1	1.3	1.9	0.1	0.0	48.5	<5	Unobj	Unobj	2.0	30.0	0	0	31372
Minimum1		0.00	0.00	0.82	18.20	0.00	0.90	0.00	1.16	0.19	14.80	0.11	0.10	0.50	0.08	0.00	-18.10	0.00	0.01	0.01	0.10	28.00	0.00	0.00	17.80
Maximum0		0.00	0.24	5.80	389.10	1.30	3.10	150.00	31.50	7.00	350.60	40.80	9.00	5.50	0.32	0.03	373.50	0.00	0.01	0.01	7.00	30.00	4.00	10.00	31372.00
Mean1		0.00	0.04	2.37	111.06	0.36	1.73	41.08	16.91	3.18	144.53	6.64	2.70	2.08	0.17	0.01	91.89	#DIV/0!	0.01	0.01	2.03	28.78	0.14	0.43	919.12
SD7		0.00	0.05	1.07	67.69	0.34	0.55	42.08	6.90	1.80	69.08	8.32	2.23	1.20	0.07	0.01	69.46	#DIV/0!	0.00	0.00	2.13	0.51	0.61	1.81	4426.51
NSDWQ 20152		0.001	0.02	5	300	0.5-2.5	200	"-"	75	"-"	"-"	250	0.7	"-"	"-"	0.2	"-"	5	Unobj	Unobj	#REF!	AMBIENT	0	10	

Zones outside of the argillaceous sediment-enriched EAG Formation that have high aquifer resistivities are characterized by low TDS (50 mg/l) and EC (120 S/cm) values, and vice versa. These low resistivity regions are a result of the dissolution of some minerals, like gypsum and halite, which have led to a rise in the overall solute concentration. The NSDWQ (2015) standard color is 5.00 Pt-Co, which is in line with the water color values, which were all around 5 Pt-Co. The amount of clay minerals, ferruginous substances, and schists that have dissolved in the groundwater was thought to be the cause of these variances. The high values of colour, EC, pH, and TDS in some parts of the study area are indicators of the abundant free ions present in the water. This can be attributed to the dissolution between water and existing soluble rock masses (Hem 1989). The concentrations of cations: Na^{+}, Ca^{2+}, K^{+}, Mg^{2+}, Mn^{2+}, and Zn Vary, respectively, from 0.9–3.1, 1.16–31.5, 0.5–5.5, 0.01–40.30, 0.00–0.03, and 0.05–1.50 mg/l (Table 2). Increase in the concentrations of Na^{+}, Ca^{2+}, and Mg^{2+} was traceable to dominant ionic compositions of major rock types in the sedimentary formations present in the area (Figs. 1b, 6). Since the different aquifer strata and the materials that make up their vadose zone are rich in silicate minerals, the groundwater is able to absorb large amounts of Ca^{2+}, Mg^{2+}, and Na^{+}, which are likely byproducts of calcite and silicate weathering processes (Holland 1978; Hem 1989). The low potassium ion content in groundwater may be caused by the K-feldspathic-enriched rocks' resistance to weathering (Kolahchi and Jalali 2006; Uquetan et al 2017). The chemistry of the groundwater system is changed by the interaction of carbonate rocks with groundwater (percolating and water moving inside aquifers). Other processes, like dolomitization, albitization of feldspars, and cation exchange in clay minerals, also include the interaction of aquifer water and rock. Calcite ($CaCO_3$) and dolomite ($CaMg(CO_3)^2$), two minerals found in rocks and soils, are potential sources of such cation concentrations in groundwater (Younger 2007). Similar occurrences of increased concentration of these cations in other areas of the Mamfe Embayment and Benue Trough have also been documented by Akpan et al. (2013) and Tijani (2004), respectively. Other factors that contribute to elevated cation concentration in groundwater include composts, pesticides, herbicides, and soil fumigants as well as the careless disposal of industrial waste water and the application of chemicals that improve soil fertility, such as NPK [nitrogen (15%), phosphorus (30%), and potassium (55%)]. If the materials in the vadose zone are unable to naturally attenuate the vertical flow of such contaminants, such chemicals are capable of flowing through preferential pathways in the vadose zone (Akpan et al. 2014). Cl-, HCO_3-, NO_3^{2-}, NO_2^{2-}, SO_4^{2-}, and PO_4^{3-} concentrations varied from 0.00 to 1.30, 14.80 to 350.0, 0.82 to 5.82, 0.01-0.60, 0.60-81.20, and 0.1 to 9.0 mg/l, respectively (Table 3 a & b). Low NO_3 values were linked to the area's predominate denitrification process (Akpan et al. 2014). The most predominant ions are Cl^{-} and HCO_3^{-}, and their quantity reveals the different causes of salinization (Akpan et al. 2013).

Table 4 Pearson CORRELATION MATRIX of Chemical constituents of groundwater in some urban communities in Cross River State

	pH	NO2	EC	TDS	BOD	DO	SO4	Zn	Al	Ba	Cr	Cd	Cu	F	Fe	Pb	Mg	Ni	NO_3^+	$CaCO_3$	Na	Ca	NaCl	HCO_3-	Cl	PO4	X	NH4	CO3	Turbidity	Temperature
pH		0.17	0.41	0.37	0.77	0.19	0.00	0.01	0.64	0.68	0.74	0.70	0.59	0.71	0.01	0.07	0.45	0.04	0.14	0.03	0.17	0.28	0.84	0.85	0.91	0.51	084	0.44	0.06	0.12	0.32
NO2	0.20		0.26	0.89	0.23	0.12	0.07	0.01	0.54	0.01	0.36	0.15	0.02	0.10	0.23	0.01	0.43	0.08	0.22	0.18	0.57	0.62	0.19	0.87	0.55	0.88	0.16	096	007	0.01	0.04
EC	-0.12	0.16		0.28	0.64	0.57	0.75	0.93	0.48	0.08	0.14	0.70	0.23	0.06	0.80	0.27	0.16	0.06	0.00	0.35	0.01	0.40	0.24	0.32	0.53	0.72	0.54	023	0.74	0.62	091
TDS	0.13	0.02	0.16		0.06	0.08	0.15	0.59	0.53	0.54	0.37	0.79	0.35	0.58	0.79	0.70	0.77	0.68	0.85	0.12	0.62	0.82	0.51	0.68	0.03	0.26	0.51	094	0.3	O.68	0.92
BOD	-0.04	-0.18	-0.07	0.27		0.48	0.51	0.11	0.75	0.03	0.85	0.18	0.14	0.52	0.62	0.85	0.63	0.12	0.91	0.38	0.77	0.43	0.28	0.31	0.01	0.33	0.74	0.64	038	0.04	0.06
DO	-0.19	-0.22	0.08	0.26	-0.10		0.21	0.26	0.79	0.03	0.48	0.74	0.52	0.28	0.80	0.19	0.32	0.12	0.89	0.60	0.24	0.14	0.64	0.87	0.55	0.87	0.60	0.06	0.68	0.13	0.65
SO4	0.41	0.26	-0.05	0.21	-0.10	0.18		0.01	0.76	0.20	0.88	0.09	0.19	0.64	0.93	0.05	0.53	0.21	0.11	0.36	0.84	0.50	0.68	0.69	0.66	0.25	0.87	0.24	033	0.23	0.03
Zn	0.38	0.37	0.01	0.08	-0.23	0.16	0.38		0.99	0.00	0.86	0.00	0.02	0.27	0.01	0.00	0.18	0.01	0.00	0.09	0.50	0.23	0.59	0.63	0.70	0.84	0.90	0.55	0.05	0.00	0.44
Al	0.07	0.09	0.10	-0.69	-0.05	0.04	-0.04	0.00		0.10	0.65	0.28	0.97	0.52	0.89	0.88	0.73	0.49	0.59	0.86	0.01	0.64	0.52	0.02	0.44	0.35	0.83	0.62	0.80	0.32	0.59
Ba	0.06	0.36	0.25	0.09	-0.30	0.32	0.18	0.59	0.23		0.18	0.00	0.00	0.85	0.04	0.00	0.15	0.01	0.07	0.07	0.03	0.12	0.80	0.75	0.34	0.17	0.75	0.62	0.01	0.00	0.42
Cr	0.05	0.13	0.21	-0.13	-0.03	0.10	-0.02	0.03	-0.07	0.19		0.09	0.82	0.13	0.90	0.27	0.35	0.35	0.71	0.63	0.50	0.63	0.12	0.75	0.95	0.87	0.09	0.83	088	0.87	0.97
Cd	0.26	-0.21	-0.06	0.04	0.19	-0.05	0.25	-0.51	-0.16	-0.48	-0.25		0.14	0.25	0.03	0.45	0.73	0.11	0.00	0.27	0.11	0.48	0.43	0.73	0.80	0.10	0.76	0.22	022	0.00	0.64
Cu	-0.08	0.32	0.17	0.14	-0.21	-0.09	0.19	0.34	0.40	0.47	0.03	-0.22		0.38	0.97	0.06	0.38	0.23	0.50	0.52	0.79	0.67	0.16	0.64	0.89	0.26	0.3	0.96	019	0.00	0.86
F	0.05	-0.24	0.27	0.78	0.09	0.16	0.07	-0.16	0.09	0.03	-0.22	0.17	0.13		0.36	0.97	0.09	0.24	0.21	0.51	0.09	0.58	0.48	0.90	0.76	0.10	0.29	0.23	054	0.00	0.47
Fe	0.36	0.18	0.04	-0.04	-0.07	0.04	-0.01	0.38	0.02	0.29	0.02	-0.31	-0.01	-0.13		0.07	0.39	0.15	0.05	0.44	0.44	0.48	0.77	0.89	0.31	0.10	0.48	0.20	037	0.01	0.43
Pb	-0.26	-0.39	-0.16	-0.06	-0.03	-0.19	-0.28	-0.52	-0.02	-0.47	-0.16	0.11	-0.27	-0.01	-0.26		0.35	0.02	0.67	0.54	0.32	0.51	0.99	0.61	0.67	0.27	0.74	0.87	0.79	0.00	0.58
Mg	-0.11	-0.11	-0.20	-0.04	-0.07	-0.14	-0.09	-0.20	-0.05	-0.21	0.64	0.05	-0.13	-0.25	-0.13	0.14		0.73	0.53	0.74	0.45	0.01	0.81	0.82	0.72	0.22	0.40	0.55	052	0.05	0.45
Ni	-0.30	-0.25	-0.27	-0.06	0.23	-0.22	-0.18	-0.38	-0.60	-0.39	-0.14	0.23	-0.18	-0.17	-0.21	0.33	0.05		0.91	0.15	0.19	0.98	0.24	0.40	0.69	0.07	0.93	0.70	0.13	0.00	0.36
NO3-	0.30	-0.18	0.47	-0.03	0.02	0.02	-0.23	-0.49	-0.08	-0.26	0.55	0.40	-0.10	0.48	-0.28	0.06	0.09	0.02		0.06	0.17	0.46	0.29	0.73	0.37	0.90	0.47	0.08	0.06	0.00	0.50
CaCO3	-0.21	-0.19	0.14	-0.23	0.13	-0.08	-0.14	-0.24	0.03	-0.26	0.07	0.16	-0.10	0.10	-0.12	-0.09	0.05	0.21	0.28		0.94	0.79	0.70	0.02	0.87	0.62	0.06	0.63	0.00	0.07	0.04
Na	-0.32	0.08	0.38	0.07	0.04	0.17	-0.03	0.10	0.36	0.32	0.10	-0.23	-0.04	0.25	0.11	-0.14	-0.11	-0.19	0.20	-0.01		0.22	0.07	0.05	0.24	0.07	0..67	0.38	0.99	0.13	0.54
Ca	0.20	0.07	-0.12	-0.33	0.11	0.21	0.81	0.17	-0.07	0.23	-0.07	0.10	0.06	0.08	-0.10	-0.10	-0.35	0.00	-0.11	-0.04	-0.18		0.44	0.84	0.13	0.89	0.34	0.84	0.33	0.14	0.23
NaCl	-0.16	-0.19	0.17	-0.10	0.16	-0.07	-0.06	-0.08	-0.10	0.04	0.23	-0.11	0.20	0.10	0.04	0.00	0.03	0.17	0.16	0.06	0.26	-0.11		0.98	0.72	0.91	0.68	0.86	0.68	0.81	0.06
HCO3-	0.03	0.02	0.15	-0.06	0.15	0.02	-0.06	-0.07	0.34	-0.05	0.65	-0.05	-0.07	0.52	-0.02	-0.07	0.03	-0.12	0.05	0.33	0.28	-0.03	0.00		0.05	0.45	0.29	0.28	0.02	0.84	0.14
Cl	0.02	-0.09	-0.09	0.31	0.38	-0.09	-0.06	-0.06	-0.11	-0.14	-0.01	0.04	0.02	0.04	-0.15	-0.06	0.05	0.06	0.13	0.02	0.17	0.22	0.05	-0.60		0.19	0.52	0.42	0.88	0.B	0.31
PO4	0.10	-0.02	0.05	-0.16	-0.14	-0.02	-0.17	-0.03	0.14	0.20	0.02	-0.24	-0.16	0.24	0.24	0.16	-0.18	-0.26	-0.02	-0.07	0.26	-0.02	-0.02	-0.11	-0.19		0.19	0.94	0.68	0.22	0.26
X	0.03	0.20	-0.09	0.10	-0.05	0.08	-0.02	0.02	-0.03	-0.05	-0.25	0.05	-0.22	-0.15	0.10	-0.05	-0.12	-0.01	-0.11	-0.27	-0.06	0.14	-0.06	-0.15	0.09	-0.19		0.89	0.09	1.00	0.92
NH4	0.11	-0.01	0.18	-0.01	-0.07	0.28	-0.17	-0.09	0.07	0.07	0.03	0.18	0.00	0.17	0.19	-0.02	-0.09	-0.06	0.25	-0.07	0.68	0.03	0.03	0.16	0.12	-0.01	-0.02		055	0.94	0.28
CO3	-0.28	-0.26	0.05	-0.20	0.13	-0.06	-0.14	-0.28	0.04	-0.35	0.02	0.18	-0.19	0.09	-0.13	-0.04	0.09	0.22	0.27	0.99	0.00	-0.14	0.06	0.32	0.02	-0.06	-025	-0.09		0.03	0.02
Turbidity	0.22	0.38	0.07	0.06	-0.30	0.22	0.17	0.82	0.14	0.78	-0.02	-0.52	0.40	0.06	0.38	-0.48	-0.28	-0.45	-0.44	-0.26	0.22	0.21	-0.04	-0.03	-0.18	0.18	0.00	0.01	-030		0.43
Temperature	0.14	0.30	0.02	-0.01	-0.27	0.07	0.30	0.11	-0.08	0.12	0.01	0.07	-0.03	0.11	0.12	0.08	-0.11	-0.13	-0.10	-0.30	-0.09	0.18	-0.27	-0.21	-0.15	0.16	-0.02	0.16	-032	0.11	

3.4. Health Survey Results

Table 5 Socio-demographic Characteristics of Infested Respondents with Water Borne Disease Intestinal Parasite

Variable	No of respondent	No infected %	P. value
Gender			007
Male	2,124	756 (55.6)	
Female	1,476	680 (460)	
Age Stratification			0.00
0 -10 years	140	65 (46.1)	
11-20 years	412	231 (56.3)	
21-30 years	1,086	664 (61.1)	
31-40 years	1,002	54 (45.3)	
41-50 years	560	130 (23.1)	
51 and above	400	40 (9.8)	
	3,600	1,584 (44)	
Education Background			0.06
No education	152	48 (29.6)	
Primary education	960	420 (43.7)	
Secondary education	1,400	702 (501)	
Tertiary education	1,078	480 (44.5)	

Table 6 Prevalence of Human Intestinal Parasites Identified

Parasites Species	Number infected	Prevalence
Entamoebahistolyfica	412	26.1
Ascarislumbricoides	340	21.5
Taeniasaginata	98	6.1
Necatoramericanus	530	33.4
Trichuristrichuira	204	12.9
	1,584	440

Out of 3600 persons examined, 1,584 (44.02) were infected. The prevalence was higher in females (46.0%) than males (35.6%) the age group with the highest prevalence (61.1%) was 21-30 years followed by the age group of 11-20 years with a prevalence of (56.3) then age group 0-10 years (46.1%), thereafter followed by the age group of 31-40 years (45.3%) and the least prevalence was from age group 50 and above with a prevalence of 9.8%. there was no significant difference (P=0.00) in prevalence between the age groups. Education status related prevalence revealed highest prevalence among those in the secondary school (50.1) followed by those in the tertiary education education level (44.5%) closely behind was those at the primary school (43.7%) and the non-education group has the least prevalence of (29.6%).

3.5. Drinking water quality health impact assessment

The hardness of water will determine how it is used for drinking and domestic uses (Karanth 1987). If carbonate and bicarbonate are present, water hardness may be temporary, but if calcium and magnesium sulfates and chlorides are present, it may be permanent (Fig.3). Due to the presence of siltstones and other calcic and dolomitic elements in the vicinity, the high amounts of calcium and magnesium can be linked to them (Ebong et al. 2014; Haritash et al. 2008; Uquetan et al 2020). According to Schroeder (1960), hard water increases the need for detergents to foam and may contribute to various cardiac ailments. The WHO-desirable level for total drinking water hardness is 100 mg/l, whereas the highest allowable limit is 500 mg/l. According to Sawyer and McCarthy's (1967) TH classification, groundwater sampling stations with total hardness values greater than 120 mg/L, or 24.5%, are hard; those with values between 83 and 120 mg/L, or 24.5%; and others with values lower than 83 mg/L, or 51%; are moderately hard (Table 3). The level of TDS, which should be less than 500 mg/l, will determine whether groundwater is suitable for any purpose (Freeze and Cherry 1979; Adedokkun et al 2021).

3.6. Recommended aquifer management practices

The following aquifer management practices have been recommended to engender good groundwater quality in the area.

- In the low-lying northern zones, the use of inorganic chemical fertilizers, especially those enhanced with nitrogenous substances, should be properly monitored. This strategy is the most practicable and accepted standard practice for reducing groundwater pollution brought on by the use of fertilizers in places with shallow aquifers.
- Carefully consider when to apply inorganic fertilizers so that it does not coincide with the area's highest period of leaching, which will also be the region's peak period of rainfall (June and July). Therefore, fertilizer applications must be made when crop uptake is at its highest. Regulations to protect important water supply aquifers should be adopted.
- Developing wholesome hygiene practices and behaviors. Septic system management techniques, such as routine pumping and inspection (for instance, every five years), ought to be used.
- Chemicals must not be dumped on the ground or into drains. To lessen the negative effects of industrial waste on the environment, waste management strategies that are beneficial to the environment should be used, such as recycling.

4. Conclusion

To assess the vulnerability of the aquifer and the quality of the groundwater, electrical resistivity tomography was used in some areas of the study area. This was supplemented by the collection and laboratory analysis of borehole water samples to assess the quality of the groundwater and its effects on human health. The low resistivity zone (deep to light blue color), the intermediate zone (green to yellow), and the extremely high resistivity zone were discovered in the study as three different zones that were isolated from the horizontal profiling method (yellow to purple colour). The profiles' low resistivity zones are probably clay-dominated regions with minimal or no contamination. Despite the fact that the findings of the laboratory study of the borehole water (groundwater) show that the dissolve oxygen (DO) level is greater than the NSDWQ suggested value of 5.0 in all of the boreholes.

Results from electrical resistivity data were utilized to define the lithostratigraphic units, albeit they do not satisfactorily correlate with geologic logs. Based on the VES resistivity values that had previously been obtained within the study region, the quality of the groundwater was evaluated using water samples taken from 409 boreholes. The Nkporo Shale Formation, fractured sandstones, shales, and siltstones of the Eze-Aku Group, which acts as the aquifer unit with moderate groundwater supplies, were all distributed laterally and vertically according to the geophysical data. The groundwater from these aquifers exhibits dominance in Ca2+, Mg2+, and Na+, which is thought to have been caused by silicate weathering processes. These formations are known to be rich in silicate minerals. These cations maintained equilibrium while the silicate minerals were being hydrolyzed. Groundwater samples were geochemically analyzed, and the predominant water facies was calcium-magnesium-carbonate-bicarbonate. In general, local geology has an impact on the water facies of the region.

When compared to criteria for drinking water applications, the groundwater Physico-chemical analysis results were deemed to be good because they were below acceptable limits. Since the groundwater system was found to be fresh, it can be used for drinking and household uses. This method has limitations since there is a lack of hydrochemical data, despite the fact that it can produce trustworthy results that can act as the initial guide to the distribution, availability, and quality of groundwater in the area.

Compliance with ethical standards

Acknowledgments

The authors are thankful to the Cross River State Water Board Limited (CRWBL), the Cross River State Rural Water Supply and Sanitation Agency (CRS-RUWATSSA) and the Cross River State Community and Rural Development Agency (CRSCRDA) for freely releasing some of the borehole data used in this study. The authors are also thankful to the Nigeria's Tertiary Education Trustfund (TETFUND) for funding this research through approval conveyed by TETF/RD&D/CE/UNI/CAL/RG/2021/VOL.1

Disclosure of conflict of interest

No conflict of interest to be disclosed.

References

[1] Adedokun, I. O., Ogar-Abang, M. O., Egor, A. O., Osang, J. E., Akpe, R. I., Oba, J. O., Emeruwa, C., (2021) Empirical Study Of Cellular Network And Signal Strength In Calabar, Cross River State, Nigeria; International Journal of Advances in Engineering and Management (IJAEM) Volume 3, Issue 4 Apr. 2021, pp: 157-186 www.ijaem.net ISSN: 2395-5252

[2] Akpan AE, Ebong ED, Ekwok SE (2014) Assessment of the state of soils, shallow sediments and groundwater salinity in Abi, Cross River State, Nigeria. J Environ Earth Sci. doi:10.1007/s12665- 015-4014-6

[3] Akpan AE, Ebong ED, Emeka CN (2015) Exploratory assessment of groundwater vulnerability to pollution in Abi, southeastern Nigeria using geophysical and geological techniques. J Environ Monit Assess 187(4):4380. doi:10.1007/s10661-015-4380-2

[4] Akpan AE, Ugbaja AN, George NJ (2013) Integrated geophysical, geochemical and hydrogeological investigation of shallow groundwater resources in parts of the Ikom-Mamfe Embayment and the adjoining areas in Cross River State, Nigeria. J Environ Earth Sci 70:1435–1456

[5] APHA (1995) Standard methods for the examination of water and waste water, 19th edn. American Public Health Association, Washington, DC

[6] Bathrellos GD, Skilodimou HD, Kelepertsis A, Alexakis D, Chrisanthaki I, Archonti D (2008) Environmental research of groundwater in the urban and suburban areas of Attica region, Greece. Environ Geol 56(1):11–18

[7] Benkhelil J (1982) Benue trough and Benue chain. Geol Mag Niger 119:115–168

[8] Chron J Dis 12:586–591 Soupios P, Kouli M, Vallianatos F, Vafidis A, Stavroulakis G (2007) Estimation of aquifer parameters from surficial geophysical methods. A case study of Keritis Basin in Crete. J Hydrol 338:122–131

[9] Douglas EB, Leo WN (1977) Hydrogeochemical relationships using partial correlation coefficient. Water Resour Bull 13:843–846

[10] Ebong ED, Akpan AE, Onwuegbuche AA (2014) Estimation of geohydraulic parameters from fractured shales and sandstone aquifers of Abi (Nigeria) using electrical resistivity and hydrogeologic measurements. J Afr Earth Sc 96:99–109.

[11] Egor, A. O., Osang, J. E., Uquetan, U. I., Emeruwa C., Agbor, M. E. (2016) Inter-Annual Variability of Rainfall in some States of Southern Nigeria. International Journal of Scientific Technology Research. Vol. 4 Issue 10, ISSN 2277-8616 pp 134-154.

[12] Egor, A. O., Osang, J. E., Emeruwa C., Ebong, D. E., Uquetan, U. I., Bawan, A. M. (2016) Critical Study of Ground Water Potential of Obubra Local Government Area, Cross River State. International Journal of Scientific Technology Research. Vol. 4 Issue 10, ISSN 2277-8616 pp 122-126

[13] Egor, A. O., Osang, J. E., Isreal-Cookey C., Uquetan, U., Adedokun, I. O., Nwanchukwu, N. C., Ibor, I. E. (2020) Hydrodynamics Model of Temperature Variation due to Gas Flaring activities in some parts of Niger Delta Area of Nigeria; Science Arena Publications Specialty Journal of Engineering and Applied Science ISSN: 2520-5943 Available online at www.sciarena.com 2020, Vol, 5 (1): 1-9.

[14] Egor, A. O., Adedokun, I. O., Uquetan, U. I., Osang, J. E., Isreal-Cookey C, Oba, J. O. (2020) Application of Electro-Geophysical and laboratary methods in soil quality assessment for lowland rice production in Obubra local government area, cross river state; To Physics Journal Vol 6 (2020) ISSN: 2581-7396.

[15] Egor, A. O., Uquetan, U. I., Ekpo, C. M Umuji, J. I. (2020) Review of Mathematical Modelling of the Time Dependent Schrodinger Wave Equation using Different methods; Science Arena Publications Specialty Journal of Engineering and Applied Science ISSN: 2520-5943 Available online at www.sciarena.com 2020, Vol, 5 (1): 10-27.

[16] Egor, A. O., Osang, J. E., Isreal-Cookey C., Uquetan, U. I., Adedokun, I. O. ,Nwanchukwu, N. C., Ibor, I. E. (2020) Hydrodynamics Model of Temperature Variation due to Gas Flaring activities in some parts of Niger Delta Area of Nigeria. Science Arena Publications Specialty Journal of Engineering and Applied Science ISSN: 2520-5943 Available online at www.sciarena.com 2020, Vol, 5 (1): 1-9.

[17] Egor, A. O., Adedokun, I. O., Uquetan, U. I., Osang, J. E., Oba, J. O., Isreal-Cookey C (2020) Application Of Electro-Geophysical And Laboratary Methods In Soil Quality Assessment For Lowland Rice Production In Obubra Local Government Area, Cross River State; To Physics Journal https://purkh.com; 6 (6) 19 -43.

[18] Ekwueme BN (2003) The Precambrian geology and evolution of the Southeastern Nigeria basement complex. University of Calabar Press, Nigeria

[19] Ekwueme BN, Nyong EE, Petters SW (1995) Geological excursion guidebook to Oban Massif, Calabar Flank and Mamfe Embayment, Southeastern, Nigeria. Dechord Press, Calabar

[20] Eseme E, Agyingi CM, Foba-Tendo J (2002) Geochemistry and genesis of brine emanations from Cretaceous strata of the Mamfe Basin, Cameroon. J Afr Earth Sci 35:467–476

[21] Etuk EE, Ukpabi N, Ukaegbu VU, Akpabio IO (2008) Structural evolution, magmatism and effects of hydrocarbon maturation in Lower Benue Trough, Nigeria: a case study of Lokpaukwu, Uturu and Ishiagu. Pac J Sci Technol 9(2):526–532

[22] Freeze RA, Cherry JA (1979) Groundwater. Prentice Hall, Englewood Cliffs, New Jersey

[23] Gemail KS, El-Shishtawy AM, El-Alfy M, Ghoneim MF, Abd ElBary MH (2011) Assessment of aquifer vulnerability to industrial waste water using resistivity measurements: a case study, along El-Gharbyia main drain, Nile Delta, Egypt. J Appl Geophys 75:140–150

[24] Giridharan L, Venugopal T, Jayaprakash M (2008) Evaluation of the seasonal variation on the geochemical parameters and quality assessment of the groundwater in the proximity of River Cooum, Chennai, India. J Environ Monit Assess 143:161–178

[25] Gu¨ler C, Thyne GD, McCray JE, Turner AK (2002) Evaluation of graphical and multivariate statistical methods for classification of water chemistry data. Hydrogeol J 10:455–474

[26] Handa BK (1979) Groundwater pollution in India. In: Proceedings of National Symposium on Hydrology. IAHS, Publication University of Roorkee, India, pp 34–49

[27] Haritash AK, Kaushik CP, Kaushik A, Kansal A, Kumar YA (2008) Suitability assessment of groundwater for drinking, irrigation and industrial use in some North Indian villages. J Environ Monit Assess 145:397–406

[28] Hem JD (1989) Study and interpretation of the chemical characteristics of natural water, 3rd edn. US Geological Survey WaterSupply Paper 2254, p 263

[29] Holland HD (1978) The chemistry of the atmosphere and oceans. Wiley, New York, p 351 Inman JR (1975) Resistivity inversion with ridge regression. Geophysics 40:798–817

[30] Inoubli N, Gouasmia M, Gasmi M, Mharndi A, Ben Dhia H (2006) Integration of geological, hydrochemical and geophysical methods for prospecting thermal water resources: the case of the Hmeima region (central-western Tunisia). J Afr Earth Sci 46(3):180–186

[31] Interciencia, Escuela Ozcep F, Yıldırım E, Tezel O, Asci M, Karabulut S (2010) Correlation between electrical resistivity and soil-water content based artificial intelligent techniques. Int J Phys Sci 5(1):047–056

[32] Karanth KR (1987) Groundwater assessment development and management. Tata Mc Graw-Hill, New Delhi, p 720

[33] Ketata M, Gueddari M, Bouhlila R (2011) Suitability assessment of shallow and deep groundwaters for drinking and irrigation use in the El Khairat aquifer (Enfidha, Tunisian Sahel) Environmental. Earth Sci. doi:10.1007/s12665-011-1091-z

[34] Kolahchi Z, Jalali M (2006) Effect of water quality on the leaching of potassium from sandy soil. J Arid Environ 68:624–639

[35] Massoud U, Santos F, Khalil MA, Taha A, Abbas AM (2010) Estimation of aquifer hydraulic parameters from surface geophysical measurements: a case study of the Upper Cretaceous aquifer, central Sinai, Egypt. Hydrogeol J 18:699–710

[36] Meldrum PI, Kuras O, Wilkinson PB, Chambers JE (2008) Advances in geoelectric imaging technologies for the measurement and monitoring of complex earth systems and processes. In: Proceedings 33rd international geological congress, Oslo, Norway. August 10–14, 2008

[37] Mhamdi A, Dhahri F, Gouasmia M, Moumni L, Mohamed S (2015) Groundwater salinization survey of the Upper CretaceousMiocene Complexe terminal aquifer in the Sabaa Biar area of southwestern Tunisia. J Afr Earth Sci 112:83–92

[38] Minsley BJ, Ajo-Franklin J, Mukhopadhyay A, Morgan FD (2011) Hydrogeophysical methods for analyzing aquifer storage and recovery systems. Groundwater 49(2):250–269

[39] Murat RC (1972) Stratigraphy and paleogeography of the cretaceous and lower tertiary in southern Nigeria. In: Dessauvagie TFJ, Whiteman AJ (eds) African geology. Ibadan Univ. Press, Ibadan, pp 251–266

[40] Nguimbous-Kouoh JJ, Takougang EMT, Nouayou R, Tabod CT, Manguelle-Dicoum E (2012) Structural interpretation of the Mamfe sedimentary Basin of southwestern Cameroon along the Manyu River using audiomagnetotellurics survey. International Scholarly Research Network (ISRN) Geophysics, p 7

[41] Odigi MI (2011) Diagenesis and reservoir quality of cretaceous sandstones of Nkporo formation (campanian) southeastern Benue trough, Nigeria. J Geol Min Res 3(10):265–280

[42] Odigi MI, Amajor LC (2009) Geochemical characterization of cretaceous sandstones from the Southern Benue Trough, Nigeria. Chin J Geochem 28:44–54

[43] Odoh BI (2010) Electro-hydraulic anisotropy of fractures in parts of Abakaliki, Ebonyi State, Nigeria-using ARS method. Int Arch Appl Sci Technol 1(1):10–19

[44] Offodile ME (1975) A mineral survey of the cretaceous of the Benue Valley, Nigeria. J Cretac Res 1:101–124 Ogilvy RD, Osang, J. E, Adedokun, I. O., Isreal-Cookey C.,

[45] Okereke CS, Esu EO, Edet AE (1998) Determination of potential groundwater sites using geological and geophysical techniques in the Cross River State, Southeastern Nigeria. J Afr Earth Sci 27(1):149–16.

[46] Osang, J. E., Egor, A. O., Uquetan, U. I, Eze, B. E., Emeruwa, C., Pekene. D. B. J. (2016) Investigation of the Relative Humidity Profile Variations in Calabar, Nigeria. International Journal of Scientific & Engineering Research, Volume 7, Issue 1, January 2016., 1134 - ISSN 2229-5518 http://www.ijser.org

[47] Osang,J. E., Uquetan,U. I. , Oko,P. E., Egor,A. O., Ekwok,S. E., and Ekpo, C. M. (2017) Effect on pH Value of Rain Water and Soil Ph in River State Nigeria. Elixir International Journal Environ. & Forestry 110; 48174-48183. ISSN 2229-712X. Www.Elixirpublishers.Com.

[48] Osang, J. E, Adedokun, I. O., Isreal-Cookey C., Egor, A. O., Uquetan, U. I., Ekpo, C. M., Umuji, J. (2020) Review of Mathematical Modelling of the Time Dependent Schrodinger Wave Equation using Different methods; Science Arena Publications Specialty Journal of Engineering and Applied Science ISSN: 2520-5943 Available online at www.sciarena.com 2020, Vol, 5 (1): 10-27.

[49] Orellana E, Moony AM (1966) Master curve and tables for vertical electrical sounding over layered structures.

[50] Panagopoulos GP, Bathrellos GD, Skilodimou HD, Martsouka FA (2012) Mapping urban water demands using multi-criteria analysis and GIS. Water Resour Manage 26(5):1347–1363

[51] Papadopoulou-Vrynioti K, Alexakis D, Bathrellos GD, Skilodimou HD, Vryniotis D, Vasiliades E, Gamvroula D (2013) Distribution of trace elements in stream sediments of Arta plain (western Hellas): the influence of geomorphological parameters. J Geochem Explor 134:17–26

[52] Papadopoulou-Vrynioti K, Alexakis D, Bathrellos GD, Skilodimou HD, Vryniotis D, Vasiliades E (2014) Environmental research and evaluation of agricultural soil of the Arta plain, western Hellas. J Geochem Explor 136:84–92

[53] Petters SW (1989) A regional hydrogeological study of rural water supply options for planning and implementation of phase II rural water programme in Cross River State. Unpubl Tech Rep Submitt DFFRI. Cross River State, 97 p

[54] Petters SW, Okereke CS, Nwajide CS (1987) Geology of the Mamfe Rift, South Eastern Nigeria. In: Matheis G, Schandelmerer H (eds) Current research in African Earth Sciences. Balkema, Rotterdam, pp 299–302

[55] Pimentel D, Houser J, Preiss E, White O, Fang H, Mesnick L, Barsky T, Tariche S, Schreck J, Alpert S (1997) Water resources: agriculture, the environment, and society source: an assessment of the status of water resources. Bioscience 47(2):97–106

[56] Piper AM (1944) A graphical interpretation of water analysis. Trans Am Geophys Union 5:914–928

[57] Prasanth SVS, Magesh S, Jitheshlal KV, Chandrasekar N, Gangadhar K (2012) Evaluation of groundwater quality and its suitability for drinking and agricultural use in the coastal stretch of Alappuzha District, Kerala, India. Appl Water Sci 2:165–175. doi:10.1007/s13201-012-0042-5 Appl Water Sci (2017) 7:2463–2478 2477 123

[58] Ragunath HM (1987) Groundwater, 2nd edn. Wiley Eastern Ltd., New Delhi Raju NJ, Reddy TVK (1998) Fracture pattern and electrical resistivity studies for groundwater exploration. J Environ Geol 34(2–3):175–182

[59] Raju N J (2007) Hydrogeochemical parameters for assessment of groundwater quality in the upper Gunjanaeru River basin, Cuddapah District, Andhra Pradesh, South India. Environ Geol 52(6):1067–1074

[60] Reijers TJA (1998) The Mfamosing limestone in South-East Nigeria: Outcrop- subsurface correlation and reservoir development. J. Petroleum Geol. 21(4): 467 – 482.

[61] Reijers TJA and Petters SW (1987) Depositional environments and Diagenesis of Albian carbonates on the Calabar Flank , SE Nigeria. J. Petroleum Geol. 10: 238 – 294.

[62] Reijers TJA and Petters SW (1997) Sequence stratigraphy based on Microfacies analysis : Mfamosing limestone. Calabar Flank, Nigeria. Geol. En Mijnbouw, 76: 197 – 215.

[63] Richards LA (1954) Diagnostics and improvement of saline and alkaline soils. US Dept. of Agriculture hand book no. 60. US Salinity Laboratory, Washington, DC

[64] Sakthimurugan S (1995) Hydrogeological studies and simulation of contaminant migration in and round Dindigul, Anna district, Tamil Nadu. Ph.D Thesis (unpublished), M.S. University, Tirunelveli, p 214

[65] Samsudin AR, Haryono A, Hamzah U, Rafek AG (2007) Salinity mapping of coastal groundwater aquifers using hydrogeochemical and geophysical methods: a case study from north Kelantan. Environ Geol, Malaysia. doi:10.1007/s00254-007-1124-9

[66] Sawyer GN, McCartly DL (1967) Chemistry of sanitary engineers, 2nd edn. McGraw Hill, New York, p 518

[67] Sawyer GN, McMcartly DL, Parkin GF (2003) Chemistry for environmental engineering and science, 5th edn. McGraw Hill, New York Schroeder HA (1960) Relations between hardness of water and death rates from certain chronic and degenerative diseases in the United States.

[68] Srinivasamoorthy K, Gopinath M, Chidambaram S, Vasanthavigar M, Sarma VS (2014) Hydrochemical characterization and quality appraisal of groundwater from Pungar sub basin, Tamilnadu, India. J of King Saud Univ Sci 26(1):37–52

[69] Subba Rao N (2002) Geochemistry of groundwater in parts of Guntur district Andhra Pradesh, India. Environ Geol 41:552–562

[70] Tijani MN (2004) Evolution of saline waters and brines in the BenueTrough, Nigeria. J Appl Geochem 19:1355–1365 Todd DK, Mays LW (2005) Groundwater hydrology, 3rd edn. Wiley, New York, p 636.

[71] Uquetan, U. I., Egor, A. O., Osang, J. E., Emeruwa C. (2016) Emperical Study of Wind Energy Potential Calabar, Cross River State. International Journal of Scientific Technology Research. Vol. 4 Issue 10, ISSN 2277-8616 pp 113-121.

[72] Udoimuk, A. B., Osang, J. E., Ettah, E. B., ,Ushie, P. O., Egor, A. O., Alozie, S. I. (2014) An Empirical Study Of Seasonal Rainfall Effect In Calabar, Cross River State, Nigeria.; Iosr Journal Of Applied Physics (Iosr-Jap) E-Issn: 2278-4861. Volume 5, Issue 5, Pp 07-15 Www.Iosrjournal.Org.

[73] Uquetan, U. I., Abua, M. A., Essoka, P. A., Osang, J. E., Egor, A. O. (2016) Pedological Study Of Soils Developed From Cretaceous Sediments Of Eze-Aku Shale Group In Yala Local Government Area, Cross River State, Nigeria;

International Journal Of Scientific & Engineering Research, Volume 7, Issue 1, Pp1120-1133, ISSN 2229-551 http://www.ijser.org.

[74] Uquetan, U. I, Essoka, P. A, Egor, A. O, Osang, J. E, Bawan A. M; A. (2016) Case Study Of The Effects Of Oil Pollution On Soil Properties And Growth Of Tree Crops In Cross River State, Nigeria; International Journal Of Scientific & Engineering Research, Volume 7, Issue 1, Pp1145-1156, ISSN 2229-551. Http://Www.Ijser.Org.

[75] Uquetan, U. I, Amah, A. E, Igelle, E.I, Egor, A. O., Ekpo, C. M. and Osang, J. E. (2017) Effect of Traffic Density on Soil along Nwanga-Ekoi- Mfamosing Road Cross River State, Nigeria. Elixir International Journal Environ. & Forestry 110 (2017) 48162-48167. ISSN 2229-712X. Www.Elixirpublishers.com.

[76] Uquetan, U. I., Igelle, E.I., Egor, A. O. , Inah, E. O, Osang, J. E., And Ekpo, C. M. (2017) Impacts Of Climate Variables On Water Yield In Ujama Okpauku River, Yala Lga, Cross River State, Nigeria. Elixir International Journal Environ. & Forestry 110 (2017) 48168-48173. ISSN 2229-712X. Www.Elixirpublishers.Com.

[77] Uquetan U. I.1, Eze E. B., Uttah C.., Obi E. O., Egor A. O., Osang J. E. (2017) Evaluation of Soil Quality in Relation to Landuse Effect in Akamkpa, Cross River State, Nigeria. Science and Education Publishing Journal, Applied Ecology and Environmental Sciences, Vol. 5, No. 2, Pp. 35-42. http://pubs.sciepub.com.

[78] Uquetan U. I., Osang J. E., EgorA. O., EssokaP. A., Alozie S. I., Bawan A. M., (2017) A Case Study of the Effects of Oil Pollution on Soil Properties and Growth of Tree Crops in Cross River State, Nigeria; International Research Journal of Pure and Applied Physics; Published by European Centre for Research Training and Development UK (www.eajournals.org) Vol.5, No.2, pp.19-28.

[79] Ushie, P. O., Ojar, J. U., Egor, A. O., Ohakwere-Eze, M. C., Osang, J. E. Alozie, S. I. (2014) Investigation Of The Efficiency Of Olive Oil As Dielectric Material And Its Economic Value On The Environment Using Its Dielectric Properties;International Journal Of Applied Physics; Www/Ijoarap.Org .

[80] Ukaegbu V. U, Akpabio IO (2009) Geology and stratigraphy of middle cretaceous sequences Northeast of Afikpo Basin, Lower Benue Trough, Nigeria. Pac J Sci Technol 103:518-256

[81] Vender Velpen BPA (1988) A computer processing package for D.C. Resistivity interpretation for an IBM compatibles, ITC JouR, Vol. 4, The Netherlands

[82] Wallace JS (2000) Increasing agricultural water use efficiency to meet future food production. J Agric Ecosys Environ 82:105–119

[83] WHO (2010) Drinking water standards, monitoring and reporting, vol 1, recommendations, 2nd edn. WHO, Geneva, p 130

[84] Wilcox LV (1948) The quality of water for irrigation uses. US Dept. Agri. Tech. Bull. 962. USDA, Washington, DC

[85] Wilcox LV (1955) Classification and use of irrigation waters. USD Circular No. 969, p 19

[86] Younger PL (2007) Groundwater in the environment: An introduction. Blackwell Publishing, Mal.